Picosecond tryptophan fluorescence of thioredoxin: Evidence for discrete species in slow exchange

ARTICLE *in* BIOCHEMISTRY · MAY 1989

Impact Factor: 3.02 · DOI: 10.1021/bi00434a038 · Source: PubMed

4 AUTHORS, INCLUDING:

Fabienne Merola
Université Paris-Sud 11
58 PUBLICATIONS **883** CITATIONS
SEE PROFILE

Rudolf Rigler
Karolinska Institutet
240 PUBLICATIONS **11,301** CITATIONS
SEE PROFILE

Jean Claude Brochon
Ecole normale supérieure de Cachan
42 PUBLICATIONS **1,501** CITATIONS
SEE PROFILE

Loeb, L. A., & Preston, B. D. (1987) *Annu. Rev. Genet. 20*, 201–230.
Otting, G., Widmer, H., Wagner, G., & Wuthrich, K. (1986) *J. Magn. Reson. 66*, 187–193.
Patel, D. J., Kozlowski, S. A., Nordheim, A., & Rich, A. (1983) *Proc. Natl. Acad. Sci. U.S.A. 79*, 1413–1417.
Plateau, P., & Gueron, M. (1982) *J. Am. Chem. Soc. 104*, 7310–7311.
Sagher, D., & Strauss, B. (1983) *Biochemistry 22*, 4518–4526.
Scheek, R. M., Boelens, R., Russo, N., van Boom, J. H., & Kaptein, R. (1984) *Biochemistry 23*, 1371–1376.
Shaka, A. J., Keeler, J., Frenkiel, T., & Freeman, R. (1983) *J. Magn. Reson. 52*, 335–338.
States, D. J., Haberkorn, R. A., & Ruben, D. J. (1982) *J. Magn. Reson. 48*, 286–292.
Takeshita, M., Chang, C. N., Johnson, F., Will, S., & Grollman, A. P. (1987) *J. Biol. Chem. 262*, 10171–10179.
Weiss, B., & Grossman, L. (1987) *Adv. Enzymol. 60*, 1–34.
Weiss, M. A., Patel, D. J., Sauer, R. T., & Karplus, M. (1984) *Proc. Natl. Acad. Sci. U.S.A. 81*, 130–134.
Zagorski, M. G., & Norman, D. G. (1989) *J. Magn. Reson.* (in press).

Picosecond Tryptophan Fluorescence of Thioredoxin: Evidence for Discrete Species in Slow Exchange†

Fabienne Mérola,‡,§ Rudolf Rigler,‡ Arne Holmgren,*,‖ and Jean-Claude Brochon§

Departments of Medical Biophysics and Physiological Chemistry, Karolinska Institutet, Box 60400, S-10401 Stockholm, Sweden, and Laboratoire pour l'Utilisation du Rayonnement Electromagnétique, CNRS–MEN–CEA, Bat. 209D, Université Paris Sud, F-91405 Orsay, France

Received August 11, 1988; Revised Manuscript Received December 20, 1988

ABSTRACT: The steady-state tryptophan fluorescence and time-resolved tryptophan fluorescence of *Escherichia coli* thioredoxin, calf thymus thioredoxin, and yeast thioredoxin have been studied. In all proteins, the tryptophan residues undergo strong static and dynamic quenching, probably due to charge-transfer interactions with the nearby sulfur atoms of the active cysteines. The use of a high-resolution photon counting instrument, with a time response of 60 ps full width at half-maximum, allowed the detection of fluorescence lifetimes ranging from a few tens of picoseconds to 10 ns. The data were analyzed both by classical nonlinear least squares and by a new method of entropy maximization (MEM) for the recovery of lifetime distributions. Simulations representative of the experimental data were used to test the MEM analysis. Strong support was obtained in this way for a small number of averaged discrete species in the fluorescence decays. Wavelength studies show that each of these components spreads over closely spaced excited states, while the temperature studies indicate that they do not exchange significantly on the nanosecond time scale. The oxidized form of thioredoxin is characterized by a high content of a very short lifetime below 70 ps, the amplitude of which is sharply decreased upon reduction. On the other hand, the fluorescence anisotropy decays indicate that reduction causes an increase of the very fast tryptophan rotations in an otherwise relatively rigid structure. While the calf thymus and *E. coli* proteins have mostly similar dynamical fluorescence properties, the yeast thioredoxin differs in many respects.

Thioredoxin is a small (M_r 11 700), ubiquitous protein with a redox-active cystine in its oxidized form, Trx-S_2.[1] Reduction of Trx-S_2 by NADPH and thioredoxin reductase gives the reduced form Trx-$(SH)_2$ with a dithiol. Thioredoxin functions in many important biological processes as an enzyme catalyzing dithiol–disulfide exchange with proteins (Gadal et al., 1983; Holmgren, 1985; Holmgren et al., 1986). Thioredoxin from *Escherichia coli* is the best characterized molecule, with its amino acid sequence of 108 residues known (Holmgren, 1968) and the three-dimensional structure of Trx-S_2 solved by X-ray crystallography to 2.8-Å resolution (Holmgren et al., 1975). The molecule has a high content of secondary structure, with five strands of β-pleated sheet and four α-helices, and the active site located in a protruding part of the structure. From the homology of primary structures, all cellular thioredoxins probably share this common fold as well as the conserved sequence of its 14-membered active disulfide ring: Trp31-Cys-Gly-Pro-Cys-Lys36 (Holmgren, 1985; Gleason & Holmgren, 1988).

The structure of Trx-$(SH)_2$ is less well-known since it has not been crystallized. Reduction does not bring significant changes in the UV absorption spectra, the ORD, and the CD spectra in the far UV (Stryer et al., 1967; Reutimann et al., 1981), while it gives a 3-fold increase in the tryptophan fluorescence emission (Stryer et al., 1967; Holmgren, 1972;

† Work supported by grants from the Swedish National Science Research Council (K-KU 3167-303) and the Swedish Medical Research Council (13X-3529). F.M. was the recipient of a postdoctoral grant from the Wenner-Gren Foundation (Sweden) during her stay at the Karolinska Institute.

* To whom correspondence should be addressed.
‡ Department of Medical Biophysics, Karolinska Institutet.
§ CNRS–MEN–CEA.
‖ Department of Physiological Chemistry, Karolinska Institutet.

[1] Abbreviations: FWHM, full width at half-maximum; MEM maximum entropy method; Trx-S_2, Trx-$(SH)_2$, the oxidized and the reduced forms, respectively, of thioredoxin; NADPH, nicotinamide adenine dinucleotide phosphate (reduced); DTT, dithiothreitol; ORD optical rotatory dispersion; CD circular dichroism; UV ultraviolet; NMR, nuclear magnetic resonance; DTNB, 5,5′-dithiobis(2-nitrobenzoic acid); NATA, *N*-acetyltryptophanamide; Boc, *tert*-butyloxycarbonyl; NHMe, methylamide.

0006-2960/89/0428-3383$01.50/0

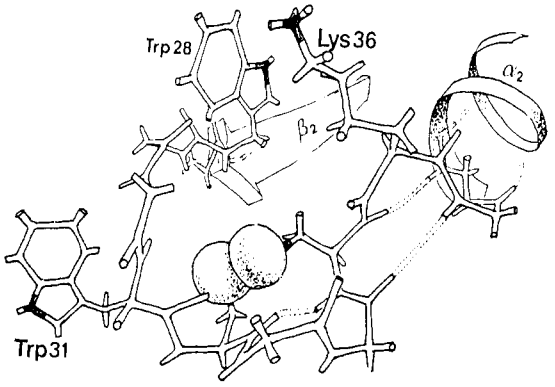

FIGURE 1: Local three-dimensional structure around the active site of oxidized *E. coli* thioredoxin from X-ray crystallography at 2.8-Å resolution (Holmgren et al., 1975).

Table I: Partial Amino Acid Sequences around the Active Site of Thioredoxins

source	no.	partial sequence	no.
E.coli [a]	25	V D F W A E W C G P C K M I A P	40
Calf thymus[b]	24	V D F S A T W C G P C K M I K P	39
Yeast [c]		Y A T W C G P C K M I A P	

[a] From Holmgren (1968). [b] From Holmgren et al. (1989). [c] From Hall et al. (1971).

Reutimann et al., 1981), a shift of one of the two NMR peaks of the indole NH protons (Holmgren & Roberts, 1976), and small changes in the near-UV aromatic region of the CD spectra (Reutimann et al., 1981). The disulfide bridge has been previously suggested as a strong quencher of the tryptophan fluorescence in Trx-S_2 (Holmgren, 1972), and the reduction to Trx-$(SH)_2$ was shown to normalize the fluorescence of mainly Trp-28, suggesting a localized conformational change affecting this residue (Holmgren, 1973, 1981). Recently, the structural differences between *E. coli* Trx-S_2 and Trx-$(SH)_2$ were studied by two-dimensional high-resolution ^{1}H NMR spectroscopy (Dyson et al., 1988). Sequential resonance assignments indicate only limited rearrangements: major chemical shifts were found at the active site and for a few residues in the strand β_2 immediately preceding the active-site S–S bridge, where the two tryptophan residues Trp-31 and Trp-28 are found (Figure 1). Additional resonance shifts involve residues forming a flat hydrophobic surface close to the active site.

We report here a time-resolved study at picosecond resolution of the tryptophan fluorescence of *E. coli* thioredoxin, together with those of yeast and calf thymus thioredoxins that both contain a single tryptophan residue equivalent to Trp-31 in the *E. coli* protein (Table I). The kinetic fluorescence properties of thioredoxin were found extremely complex, since four to five exponential terms had to be introduced in the least-squares analysis of the fluorescence decays. A new analysis method for the recovery of lifetime distributions, based on entropy maximization (MEM), was developed recently by Livesey et al. (Livesey & Brochon, 1987; Livesey et al., 1986, 1987). This method does not make use of a priori physical or mathematical models of the distribution and can handle both continuous and discrete lifetime distributions in a single analysis. It seems therefore well appropriate for the treatment of protein fluorescence kinetics, expected to show high levels of complexities and which for the moment is very incompletely understood on a theoretical level. The MEM analysis has allowed a new and powerful approach of the data in this particularly complex case. It has shown that a simple description of the thioredoxin fluorescence may be valid if its discrete components can be associated with distinct conformational and dynamical states of the tryptophan residues.

Experimental Procedures

Materials

E. coli thioredoxin (Holmgren & Reichard, 1967; Dyson et al., 1988), yeast thioredoxin (Gonzales Porqué et al., 1970), and calf thymus thioredoxin (Engström et al., 1974; Holmgren et al., 1989) were homogeneous preparations purified as described. Calf thymus thioredoxin contains, apart from the active-site disulfide, two additional half-cystine residues (Cys-61 and Cys-72) and was purified in its fully reduced form. Upon storage, air oxidation will result in formation of two disulfides per molecule. These oxidized preparations of the protein are here used as oxidized thioredoxin. They were subsequently reduced as described below. All thioredoxin samples were studied, except for the experiment at −5 °C, in a 50 mM Tris-HCl buffer, pH 7.5, with 0.1 mM EDTA and 0.02% sodium azide. The experiment at −5 °C was done in a 25% (w/w) mixture of glycerol with the above Tris buffer. Tryptophan and *N*-acetyltryptophanamide (NATA) were studied in a 10 mM phosphate buffer, pH 7.03 ± 0.03 at 20 °C, with 0.02% sodium azide. Due to the low fluorescence quantum yield of thioredoxin, the protein concentration was typically 130–170 μM/L in the fluorescence decay measurements. Buffers were made of highly pure carbon-filtrated Millipore water and treated with active charcoal immediately before use. The fluorescence level of the buffers was maintained in this way near 1% of the protein fluorescence, and no blank subtraction was performed. However, in the cases of the yeast and calf thymus thioredoxins, due to the low quantum yields and/or the low amount of material available, the fluorescence of the buffer amounted to a few percent of the protein fluorescence and had to be subtracted. Therefore, these samples were run before experiments through a small Sephadex G-25 column equilibrated with the freshly treated buffers, and the eluant buffer collected immediately ahead of the protein fractions was used as the blank. *E. coli* thioredoxin reductase, used for enzymatic assay of thioredoxin, was a pure preparation from the Physiological Chemistry Department (Karolinska Institute, Stockholm).

Methods

Enzymatic Assay. Activity of thioredoxin as a substrate for thioredoxin reductase was tested by using the DTNB assay (Slaby & Holmgren, 1979). No detectable loss of activity could be observed after several hours under laser excitation.

Reduction of Thioredoxin. Reduction of thioredoxin was obtained by adding a small volume of concentrated DTT to a final concentration of 3 mM. The reaction, as followed by the increase of the thioredoxin fluorescence, was complete within a few minutes. Absorption of oxidized DTT in the range 280–300 nm (Iyer & Klee, 1973) was checked to be negligible in view of the quantum yield determinations.

Absorption and Fluorescence Spectra. UV absorption spectra were recorded with a Varian Cary 118 UV–vis spectrophotometer. Fluorescence spectra were obtained with a Shimadzu RF-540 fluorometer and were not corrected for monochromator and photomultiplier efficiency. The excitation and emission bandwidths were 2 and 5 nm, respectively. The apparent relative quantum yields were evaluated on samples of optical densities about 0.1 at the excitation wavelength and

were calculated by using L-tryptophan as a standard (Φ = 0.144; Wiget & Luisi, 1978).

Pulse Fluorometry Measurements. The fluorescence decays and fluorescence anisotropy decays were obtained by using a single photon counting instrument previously described (Rigler et al., 1984, 1986). A mode-locked argon laser synchronously pumped a Rhodamine 6G dye laser (Coherent) at a 76-MHz repetition rate. The 600-nm light pulses, of 6-ps duration, of the dye laser were extracted by cavity dumping and converted to 300 nm through a KDP frequency doubler. The repetition rate of the cavity-dumped exciting pulses was 7.5877 MHz. The fluorescence of the sample through cutoff filters (Schott & Gen.), and the partially reflected laser beam, were both detected by a proximity type microchannel plate detector (R1564U Hamamatsu), showing no significant wavelength dependence of its time response (Rigler et al., 1984, 1986). Conventional fast electronics modules for photon counting were used. The full width at half-maximum of the instrumental function, corresponding to the laser pulse convoluted through detection response, was routinely 60 ps. The instrumental function $g(t)$, the unpolarized fluorescence decay $\mathrm{im}(t)$ (through a polarizer set at magic angle), the fluorescence polarized perpendicular to the exciting beam $\mathrm{ip}(t)$, and the dark current were measured sequentially during several tens of cycles and stored in groups of 2048 channels each. The time interval per channel was 21.4 ps. About 10^7 total counts were collected in 15 min for each polarized component of the fluorescence decays, giving 1–2 $\times$ 10^5 counts at the peak channel of $\mathrm{im}(t)$, depending on the kinetics.

The measured components $\mathrm{im}(t)$ and $\mathrm{ip}(t)$ are convolution products of the fluorescence decay laws $\mathrm{Im}(t)$ and $\mathrm{Ip}(t)$ with the instrumental function $g(t)$:

$$\mathrm{im}(t) = g(t) * \mathrm{Im}(t) \qquad \beta\mathrm{ip}(t) = g(t) * \mathrm{Ip}(t) \tag{1}$$

The correction factor $\beta = 0.950 \pm 0.003$, independent of the wavelength (as determined from the depolarized part of the fluorescence decays of NATA and tryptophan), compensates for the difference in detection sensitivity between the magic and the perpendicular positions of the analyzer.

A time shift had to be introduced in the analysis to account for the differences of optical pathways in the respective measurements of $g(t)$ and $\mathrm{im}(t)$, $\mathrm{ip}(t)$. From the delay measured between the partially reflected laser beam and the light scattered by nonfluorescent lipid vesicles placed in the sample compartment, this time shift was estimated to be 90 ps. However, fluctuations in the optical adjustments led to an uncertainty of less than 20 ps (one channel) on this value between experiments. Although the correct determination of this time shift was critical for the fitting of the very first data points, once these points were removed (about 10 channels on the leading edge of the thioredoxin fluorescence signal, corresponding to half the rise time), the fitted parameters, including the shortest components of the decay, were found insensitive to the small fluctuations of this time shift.

Least-Squares Analysis of the Fluorescence Decays. In the classical reconvolution and least-squares analysis (Grinvald & Steinberg, 1974; Wahl, 1979), the fluorescence decay law $\mathrm{Im}(t)$ was analyzed as the sum of an arbitrarily fixed number of discrete exponential terms

$$\mathrm{Im}(t) = A_0 \sum_1^n a_k e^{-t/\tau_k} \quad (\textstyle\sum a_k = 1) \tag{2}$$

and the minimal number n of exponentials necessary to fit the decay was determined by increasing n progressively until the residuals were apparently randomized, and the lowest possible χ^2 reached

$$\mathrm{Dev}(j) = \frac{\mathrm{im}^{\mathrm{cal}}(j) - \mathrm{im}^{\mathrm{exp}}(j)}{\sqrt{\mathrm{im}^{\mathrm{exp}}(j)}} \tag{3}$$

$$\chi^2 = \frac{1}{M - p} \sum_{j=1}^{M} \frac{(\mathrm{im}^{\mathrm{cal}}(j) - \mathrm{im}^{\mathrm{exp}}(j))^2}{\mathrm{im}^{\mathrm{exp}}(j)} \tag{4}$$

where M is the total number of observations, p is the number of fitted parameters, and $\mathrm{im}^{\mathrm{exp}}(j)$ is an estimate of the variance at the jth point. The mean fluorescence lifetime is the first-order mean: $\tau = \sum \alpha_k \tau_k$. Uncertainties on the fitted parameters, as obtained from the error matrix, were always below 5% and, thus, obviously below the fluctuations of these parameters along series of experiments.

MEM Analysis of the Fluorescence Decays. The maximum entropy method (MEM) has been previously used in the analysis of data from a wide range of techniques (Gull & Skilling, 1984a,b). Recently, the method was applied successfully to the ill-conditioned problem of inversion of Laplace transform in quasi-elastic light scattering (Livesey et al., 1986), and pulse fluorometry (Livesey et al., 1987; Livesey & Brochon, 1987). In this analysis, the fluorescence decay law was assumed to be the sum of a continuous distribution of positive exponential components:

$$\mathrm{Im}(t) = \int_0^\infty A(\tau) e^{-t/\tau}\, d\tau \tag{5}$$

The Skilling–Jaynes entropy function (Jaynes, 1983) was defined as

$$S = \int_0^\infty A(\tau) - m(\tau) - A(\tau) \log\left(A(\tau)/m(\tau)\right) d\tau \tag{6}$$

where $m(\tau)$ is the initial guess, which must be set to a flat distribution in log τ space when one has no a priori knowledge about the distribution $A(\tau)$ (Livesey & Brochon, 1987). In practice, 150 lifetime values equally spaced in logarithmic scale, ranging typically from 0.01 to 10 ns, were allowed on the time axis for the distribution $A(\tau)$. The distribution $A(\tau)$, which minimized the χ^2 and maximized the entropy function, was then searched, starting from the flat model $m(\tau)$. Previous tests of the MEM method (Vincent et al., 1988) have shown that an empirical criterion must be used to stop the analysis and avoid overfittings. On the basis of simulations representative of the thioredoxin experiments, we chose to stop the analysis when the χ^2 did not decrease by more than 2% over the next 20 iterations. The number of iterations necessary to reach this criterion is given for each reconstructed spectrum in the figure legends. This method was found to give excellent results with all kinds of synthetic lifetime distributions representative of the thioredoxin experiments and was still effective toward simulations carrying a similar level of nonrandom noise as the thioredoxin experiments. It is equivalent in its basic principle to the comparison of successive images performed by Vincent et al., since χ^2 changes only if the calculated function $\mathrm{im}^{\mathrm{cal}}(t)$ changes, i.e., if the image $A(\tau)$ is changing significantly. A more complete discussion of these methods and their design will be given elsewhere (Brochon et al., unpublished data).

The parameters of the fluorescence decays obtained through MEM are defined as follows: (a) the spectrum $A(\tau)$ is divided in an many peaks as can be clearly separated by two successive well-defined minima; (b) the average position τ_k of the peak k, in nanoseconds, is the barycenter

$$\tau_k = \sum_i A_i \tau_i / \sum_i A_i \tag{7}$$

calculated over all values of i included in the peak; (c) the

fractional area a_k is the ratio of the peak surface $\sum A_i$ over the entire surface of the spectrum. In cases where a well-defined minimum is not present, but the dissymmetry of the peak indicates that it is composed of several unresolved components, the calculated parameters are put between parentheses.

Least-Squares Analysis of the Fluorescence Anisotropy Decays. The fluorescence anisotropy decay law $r(t)$, in the case of a fluorophore rigidly fixed to a sphere of volume V, rotating at the temperature T in a homogeneous medium of bulk viscosity η, is a single-exponential function

$$r(t) = r_0 e^{-t/\theta} \tag{8}$$

where r_0 is the fundamental initial anisotropy of the fluorophore, linked to the angle between the absorption and emission dipoles, and should be close to 0.30 for tryptophan at 300-nm excitation (Valeur & Weber, 1977). The relaxation time θ is equal to the Brownian rotational correlation time of the molecule, given for a sphere by the Einstein–Stockes relation (k being Boltzmann's constant):

$$\theta = \eta V/kT \tag{9}$$

For nonspherical rotors, and in cases of more complex rotational behavior (Ehrenberg & Rigler, 1972; Wahl, 1980; Szabo, 1984), the anisotropy decay law may be expressed as the sum of several exponential terms:

$$r(t) = \sum_j r_{0j} e^{-t/\theta_j} \qquad (\sum_j r_{0j} = r_0) \tag{10}$$

For a fluorophore k present at a normalized concentration c_k, having a homogeneous chemical and dynamical behavior characterized by the fluorescence decay $\mathrm{Im}_k(t)$ and the anisotropy decay $r_k(t)$, the anisotropy decay law is given by

$$r_k(t) = \frac{\mathrm{Im}_k(t) - \mathrm{Ip}_k(t)}{\mathrm{Im}_k(t)} = \frac{D_k(t)}{\mathrm{Im}_k(t)} \tag{11}$$

where $\mathrm{Im}_k(t)$ and $\mathrm{Ip}_k(t)$ are the polarized fluorescence decay laws defined above and $D_k(t)$ represents the difference decay, as defined by Wahl (1979). Assuming that the fluorescence decay $\mathrm{Im}_k(t)$ and the anisotropy decay $r_k(t)$ are single exponentials, the rotational relaxation time θ_k is then related to the fluorescence lifetime τ_k of the fluorophore by

$$\frac{1}{\theta_k} = \frac{1}{\tau_{Dk}} - \frac{1}{\tau_k} \tag{12}$$

where τ_{Dk} is defined as the decay time of the difference $D_k(t)$.

For a mixture of fluorophores, $\mathrm{Im}(t)$ and $\mathrm{Ip}(t)$ are the sums of all participations: $c_k\mathrm{Im}_k(t)$, $c_k\mathrm{Ip}_k(t)$ of each species k to the total fluorescence decay laws. The total difference $D(t) = \mathrm{Im}(t) - \mathrm{Ip}(t)$ is thus equal to

$$D(t) = \sum_k c_k D_k(t) = \sum_k c_k \mathrm{Im}_k(t) r_k(t) \tag{13}$$

In a first approximation, the anisotropy function $r_k(t)$ was assumed to be identical for all species and was factored out

$$D(t) = r(t)\sum_k c_k \mathrm{Im}_k(t) = r(t)\mathrm{Im}(t) \tag{14}$$

In this case, the experimental function $d(t)$ is simply related to the total fluorescence decay $\mathrm{Im}(t)$ (analyzed as described above) and the anisotropy function $r(t)$ by

$$d(t) = \mathrm{im}(t) - \beta \mathrm{ip}(t) = g(t) * D(t) = g(t) * (\mathrm{Im}(t)r(t)) \tag{15}$$

and $d(t)$ was thus analyzed in a least-squares procedure for the determination of the parameters r_{0j} and θ_j of $r(t)$ (Wahl, 1979).

Such an analysis is aimed only at showing the relative changes in complexity of the anisotropy decays between different experiments, and also at reaching a good approximation of the initial anisotropy. Outside the case of a homogeneous dynamical behavior of a single fluorophore, or identical dynamical behavior of several fluorophores, the time constants and amplitudes obtained through eq 14 should not be given the respective physical meanings of correlation times and "angles of wobbling".

In Figure 9, the function $r_{\mathrm{exp}}(t)$ is defined as

$$r_{\mathrm{exp}}(t) = (\mathrm{im}(t) - \beta \mathrm{ip}(t))/\mathrm{im}(t) \tag{16}$$

which is an approximate, undeconvoluted representation of $r(t)$, valid only in the hypothesis of a homogeneous rotational dynamics of the system.

Evaluation of Static Quenching. For a fluorescent molecule with a radiative lifetime τ_0, the mean fluorescence lifetime τ is related to the quantum yield Φ by

$$\Phi = \tau/\tau_0 \tag{17}$$

When a fraction f of molecules becomes engaged in a nonfluorescent complex on the ground state (static quenching), the apparent quantum yield becomes $\Phi^{\mathrm{app}} = (1 - f)\Phi$. Therefore, the fraction f of complexed molecules is given by

$$f = 1 - \tau_0(\Phi^{\mathrm{app}}/\tau) \tag{18}$$

A similar simple relation holds in the case of a mixture of species at normalized concentrations c_k, with mean lifetimes τ_k, and respective fractions f_k of static quenching, if these species have identical radiative lifetimes and absorption coefficients. In this case, the total quantum yield $\overline{\Phi^{\mathrm{app}}}$ and the first-order mean lifetime $\bar{\tau}$ of the mixture yield the global ratio of the molecules engaged in the nonfluorescent complex C_q over the total concentration of fluorophores C_t:

$$\overline{\Phi^{\mathrm{app}}} = \sum_k c_k \Phi_k^{\mathrm{app}} = \sum_k c_k(1 - f_k)(\tau_k/\tau_0) = (1/\tau_0)\sum_k c_k(1 - f_k)\tau_k \tag{19}$$

$$\bar{\tau} = \frac{\sum_k c_k(1 - f_k)\tau_k}{\sum_k c_k(1 - f_k)} \tag{20}$$

$$\bar{f} = 1 - \tau_0(\overline{\Phi^{\mathrm{app}}}/\bar{\tau}) = 1 - \sum_k c_k(1 - f_k) = \sum_k c_k f_k = C_q/C_t \tag{21}$$

We estimated f in each sample from its mean fluorescence lifetime measured at 20 °C, $\lambda_{\mathrm{em}} \geq 345$ nm, and its fluorescent quantum yield at 20 °C. We determined the radiative lifetime τ_0 from the measured fluorescence lifetime of NATA (Table II) and from its published quantum yield of 0.14 (Werner & Forster, 1979), which gave a value of 21.9 ns, in good agreement with the radiative lifetime of 22.2 ns published by Ricci (1970) for tryptophan and a number of indole analogues. Since this radiative lifetime is found approximately constant in tryptophan analogues, oligopeptides, and proteins (Weinryb & Steiner, 1968; Werner & Forster, 1979; Burstein et al., 1973), we assumed that our measured value was also valid for the tryptophan residues of thioredoxin. The uncertainties on the computed fractions of static quenching were estimated by assuming 5% errors in the lifetimes and quantum yields and neglecting the error on the radiative lifetime τ_0.

Fluorescence Decays of NATA and Tryptophan. To obtain different constants (β, τ_0) as well as a for a check of the correct global calibration of the method, we measured the fluorescence decays of *N*-acetyltryptophanamide and tryptophan at pH 7.0,

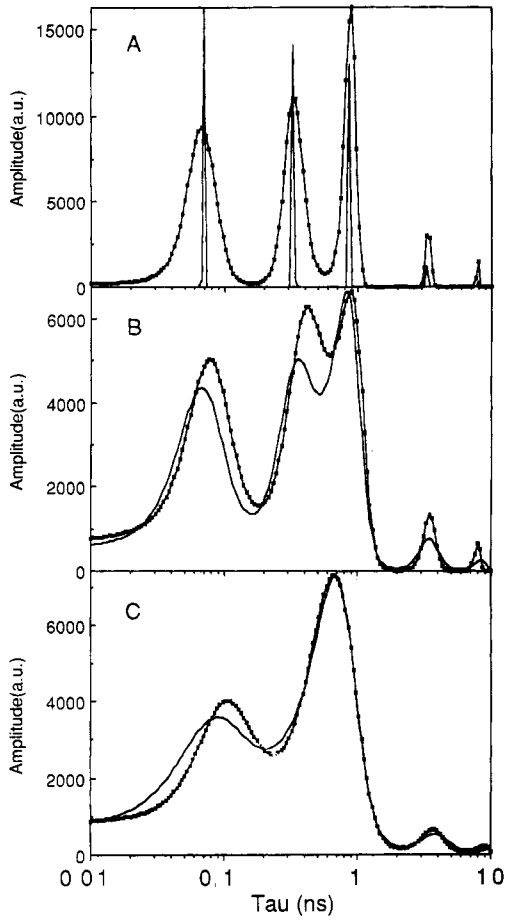

FIGURE 2: MEM analysis of different synthetic lifetime distributions compatible with the thioredoxin data (Trx-S_2, 20 °C, $\lambda \geq 370$ nm). (Smooth line) Initial distribution; (line with points) distribution recovered by MEM. (A) Five discrete exponentials, 140 iterations performed for the reconstruction. (B) Five broad distributions, 90 iterations performed. (C) Four broad distributions, 50 iterations performed. The corresponding initial and recovered parameters are tabulated in the supplementary material.

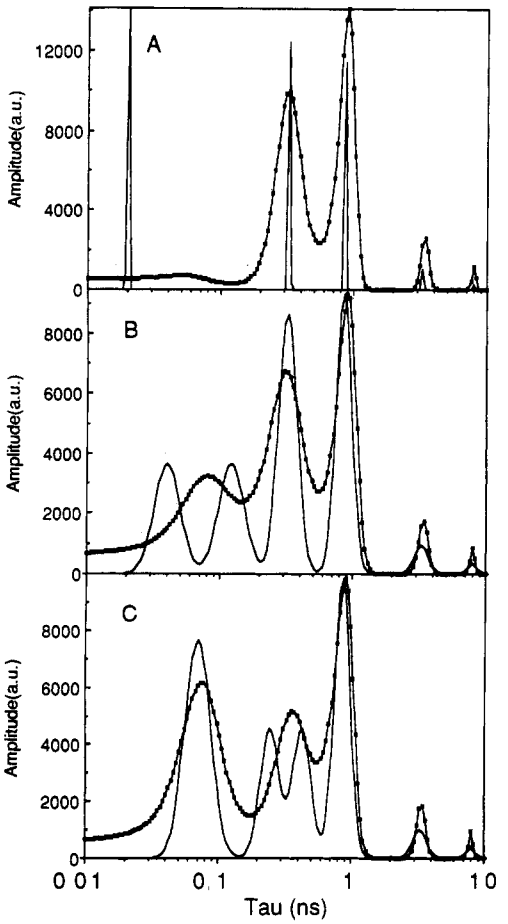

FIGURE 3: MEM analysis of different synthetic lifetime distributions for which the data do not allow complete recovery. (Smooth line) Initial distribution; (line with points) distribution recovered by MEM. (A) Short exponential term below the instrumental resolution, 90 iterations performed. (B) Unresolved peaks in the short time range, 110 iterations performed. (C) Unresolved peaks in the intermediate time range, 110 iterations performed. The corresponding parameters are tabulated in the supplementary material.

20 °C, with the same cutoff filters used in the thioredoxin measurements. These measures are in good agreement with what is known today of the fluorescence of these compounds (Petrich et al., 1983; Beechem & Brand, 1985): we found that the fluorescence decay of NATA is well described by a single-exponential function with a time constant of 3.07 ± 0.01 ns, independent of the emission wavelength; the fluorescence decays of tryptophan on the red edge of the emission spectrum ($\lambda_{em} \geq 370$ nm) are well described by a 3.2-ns component accounting for more than 99% of the decay and less than 1% of a long component around 9–10 ns. On the blue edge of the emission spectrum ($\lambda_{em} \geq 345$ nm), 5% of an additional short component of 0.7 ns is detected. NATA can be considered a good initial model for the fluorescence of tryptophan residues engaged in a polypeptide chain and exposed to water, while the higher complexity of the fluorescence decays of tryptophan has been ascribed to the different interactions of the indole ring with the ionizable groups of the tryptophan zwitterion (Szabo & Rayner, 1980).

Simulations. Synthetic decays were generated from initial lifetime distributions $A(\tau)$ reconvoluted with a measured instrumental function by the convolution routine of the least-squares and MEM analysis (Wahl, 1979). To ensure statistical accuracy representative of the thioredoxin experiments, the decays were scaled to 1.6×10^5 counts at the peak channel. To these synthetic decays was then added quasi-Gaussian noise to approximate Poisson statistics. The Gaussian noise was obtained from a VAX-780 built-in uniform generator, with additional random shuffling of the output values, and converted to a Gaussian probability distribution by use of the Box–Muller method (Press et al., 1986). To allow for comparisons, the different simulations presented here carry a constant set of about 1800 pseudorandom values giving a final absolute χ^2 of 0.99976. Simulations were also performed with several other sets of random noise, and the fluctuations in recovered MEM images for the different added noises were found negligible at the present statistical level of the simulations.

RESULTS

Simulations. We tested the ability of the MEM analysis to recover different kinds of lifetime distributions from synthetic decays (Figures 2 and 3). The tables of corresponding initial and recovered parameters are available as supplementary material. Simulations based on the fluorescence decays of *E. coli* Trx-S_2 at 20 °C are presented in Figure 2 (similar simulations were made for the reduced form). First, when the synthetic decay is generated from five discrete exponential functions with positions and weights identical with those obtained on Trx-S_2, the different components are recovered with high accuracy (Figure 2A). In Figure 2B,C are tested two other models compatible with the thioredoxin fluorescence decays. These distributions were actually obtained as successive steps in the MEM analysis of the experimental data. Figure 2C is the "first" image which gave an acceptable

Table II: Steady-State Tryptophan Fluorescence and Static Quenching in Thioredoxins at 20 °C

sample	λ_{max} (nm)	FWHM (nm)	quantum yield (%)	increase in quantum yield	mean lifetime[a] (ns)	increase in mean lifetime	fraction of static quenching (%)
tryptophan	353	63	14.4[b]		3.10		−2
NATA			14.0[c]		3.07		0
E. coli Trx-S_2	345	57	1.4		0.52		41 ± 4
E. coli Trx-$(SH)_2$	346	56	4.7	3.3	1.27	2.4	19 ± 2
calf thymus Trx-S_2	343	62	1.5		0.71		54 ± 5
calf thymus Trx-$(SH)_2$	345	60	2.2	1.5	1.04	1.5	54 ± 5
yeast Trx-S_2	348	*d*	0.7		0.34		55 ± 6
yeast Trx-$(SH)_2$	344	70	1.2	1.7	0.56	1.6	53 ± 5

[a] $\lambda_{em} \geq 345$ nm. [b] From Wiget and Luisi (1978). [c] From Werner and Forster (1979). [d] Nonmeasurable (the blue edge of the spectrum merges with the Rayleigh peak).

randomization of the residuals (i.e., a slightly less structured image could be immediately rejected upon examination of the residuals). It may therefore be regarded as the minimal structure compatible with the thioredoxin data, in which there is evidence for only four components in the spectrum. Figure 2B is an intermediate image, which gives residuals virtually undistinguishable by eye examination from those obtained in the final stage of the analysis. However, these different distributions, when used to generate synthetic decays, are relatively well recovered and clearly distinguished from each other in a MEM analysis. One should stress that simulations of this kind are undissociable from the use of MEM on real data to show that the analysis is appropriately stopped (see Experimental Procedures).

In following simulations, we tested the result of the analysis in cases where the quality of the input data forbids the complete recovery of the initial image. One of these cases may occur if the instrumental resolution is too broad to allow for the detection of a very short component. We lowered the value of the shortest lifetime of thioredoxin from 70 to 20 ps, which is of the order of the time interval per channel (21.4 ps) and approximately represents the instrumental time uncertainty of the measurements. Figure 3A shows the initial and recovered lifetime spectra when such mock data are analyzed with the MEM routine. The very short component gives rise to a broad and flat distribution with an overestimated maximum position, the weight of which is largely underestimated. Meanwhile, the relative weights and positions of the other components of the decay are correctly recovered. Because the participation of the short component to the total fluorescence signal ($c_1\tau_1$) is globaly underestimated, the mean lifetime itself is overestimated (0.67 ns instead of 0.49 ns in the initial simulation). Therefore, the short component will become partly accounted for as "static quenching".

Other cases where the true shape of the initial distribution could not be recovered are presented in Figure 3B,C. In these examples, the initial distributions include two close peaks, obtained by splitting one of the components of the thioredoxin spectrum in two peaks of equal weight separated by twice their full width. The resulting distribution thus includes six components instead of five. In both cases, the MEM analysis was unable to discriminate such closely spaced components and gave instead a broader distribution centered at the mean position of the unresolved components. The rest of the distribution was correctly recovered with, however, a general broadening of the picture.

Since this is one of the first attempts, after those of Livesey and Brochon (1987) and Vincent et al. (1988), to apply this new method on pulse fluorometry data, we will give in the following the fluorescence decay parameters obtained from both least-squares and MEM analysis.

Fluorescence Study of E. coli Thioredoxin. (*a*) *Steady-State Fluorescence Properties.* We measured the tryptophan fluorescence spectra of *E. coli* Trx-S_2 and Trx-$(SH)_2$ at 20 °C, using an excitation wavelength of 300 nm for comparisons with the time-resolved experiments (Table II). As has already been noted, the tryptophan fluorescence intensity of thioredoxin is much lower than that of aqueous tryptophan or NATA, with a quantum yield of only 1.4% in the oxidized form. The fluorescence emission is shifted by about 8 nm toward the short-wavelength range as compared to aqueous tryptophan, showing that the residues are partly shielded from interactions with the aqueous phase. On the other hand, the narrow width of the spectrum indicates that the fluorescence emissions of the two tryptophan residues are mostly superimposed and that the tyrosine contribution is negligible at this excitation wavelength.

In good agreement with previous determinations (Stryer et al., 1967; Holmgren, 1972; Reutimann et al., 1981), we observe upon reduction of *E. coli* thioredoxin a 3.3-fold increase in the steady-state quantum yield of fluorescence, while the maximum of emission and the FWHM of the spectrum do not significantly change (Table II). This is paralleled by an increase of the mean fluorescence lifetime, which is, however, of lower magnitude than the increase in steady-state intensity, suggesting that a partial static quenching of the tryptophan fluorescence is modulated by the reduction state. The fraction of tryptophan residues of *E. coli* thioredoxin engaged in a nonfluorescent complex on the ground state, as estimated from steady-state and time-resolved measurements, is shown in Table II. The tryptophan residues of both Trx-S_2 and Trx-$(SH)_2$ show high proportions of static quenching, while reduction brings a significant decrease of these static interactions.

The simulation of Figure 3A has suggested that the apparent static quenching may also include the undetected fast components of the fluorescence decay. Very weak fluorescence, due to highly efficient dynamic quenching interactions, would thus be accounted for as static quenching. However, the level of static quenching in *E. coli* Trx-S_2 decreases sharply when the temperature increases, going from 50% ± 5% at 5 °C to only 5% ± 2% at 40 °C. This is expected from the exothermic formation of a noncovalent complex, while a bimolecular collisional quenching rate would be expected on the contrary to increase (Swadesh et al., 1987). From the low value of the ratio at 40 °C, only a negligible part of the measured static quenching may actually be collisional in *E. coli* Trx-S_2.

(*b*) *Fluorescence Decays of E. coli Thioredoxin.* The fluorescence decays of *E. coli* Trx-S_2 and Trx-$(SH)_2$ are shown in Figure 4, together with the residual functions obtained in different least-squares fits of the data. The fluorescence decays of Trx-S_2 could clearly not be fitted by four experimental functions (Figure 4B). A sum of five exponential functions

Table III: Fluorescence Decay Parameters of *E. coli* Trx-S_2 at Different Emission Wavelengths, 20 °C

wavelength (nm)	lifetimes (ns) and amplitudes					mean lifetime (ns)	χ^2
	(A) Least-Squares Analysis						
≥345	0.08	0.34	0.82	2.81	6.8	0.52	1.09
	0.33	0.33	0.31	0.03	0.01		
≥370	0.07	0.34	0.86	3.18	7.8	0.51	1.14
	0.36	0.33	0.28	0.03	0.01		
≥389	0.08	0.39	0.91	3.46	9.1	0.65	1.17
	0.23	0.42	0.30	0.04	0.01		
	(B) MEM Analysis						
≥345	0.07	0.31	0.75	2.76	5.9	0.49	1.08
	0.37	0.24	0.36	0.02	0.01		
≥370	0.07	0.34	0.83	3.33	8.7	0.48	1.09
	0.38	0.30	0.29	0.02	<0.01		
≥389	0.07	0.39	0.88	3.55	9.1	0.63	1.13
	0.24	0.40	0.32	0.03	<0.01		

Table IV: Fluorescence Decay Parameters of *E. coli* Trx-$(SH)_2$ at Different Emission Wavelengths, 20 °C

wavelength (nm)	lifetimes (ns) and amplitudes				mean lifetime (ns)	χ^2
	(A) Least-Squares Analysis					
≥345	0.25	1.10	2.43	5.00	1.27	1.16
	0.37	0.34	0.25	0.04		
≥370	0.26	1.18	2.46	5.25	1.41	1.22
	0.30	0.39	0.27	0.04		
≥389	0.31	1.40	2.97	6.76	1.62	1.03
	0.20	0.57	0.21	0.02		
	(B) MEM Analysis					
≥345	0.28		(1.76)	5.12	1.24	1.10
	0.41		(0.56)	0.03		
≥370	0.27	1.26	2.56	5.43	1.40	1.09
	0.31	0.42	0.24	0.03		
≥389	0.32	1.46	3.09	7.15	1.55	0.99
	0.19	0.60	0.19	0.01		

was in all cases necessary to reach the best possible fits, with three dominant lifetimes around 0.07, 0.3, and 0.9 ns (Tables III and V). Because of the dominance of these very short components, the mean lifetime has a low value of about 0.5 ns at 20 °C, which is in keeping with the low value of the quantum yield. However, in the beginning of the decay, the deviation function could not be completely randomized with five exponential components (Figure 4C). No improvement was obtained by fitting a sixth exponential term, which resulted in a degenerated solution equivalent to five components.

The fluorescence decays of *E. coli* Trx-$(SH)_2$ are well represented, in the least-squares analysis, by sums of four exponential functions. Contrary to the oxidized form, there is no significant residual structure at short times in the deviation function (Figure 4D). Reduction results in large changes of the fluorescence composition (Tables IV and VI). Among these the most noticeable is the disappearance of the very short component at 0.07 ns, mainly to the benefit of the 3.0-ns component, therefore increasing the mean lifetime to 1.3 ns at 20 °C.

(*c*) *Wavelength Dependency of the Fluorescence Decays.* When different parts of the emission spectrum are selected with different cutoff filters ($\lambda \geq 345$ nm, $\lambda \geq 370$ nm, and $\lambda \geq 389$ nm) at 20 °C, the composition of the fluorescence decays of Trx-S_2 appears approximately constant with wavelength (Table IIIA). However, the different lifetimes increase systematically when going to the red edge of the emission. This has been observed in many proteins (Lakowicz & Cherek, 1980; Lakowicz, 1983; Gratton & Lakowicz, 1985) and was

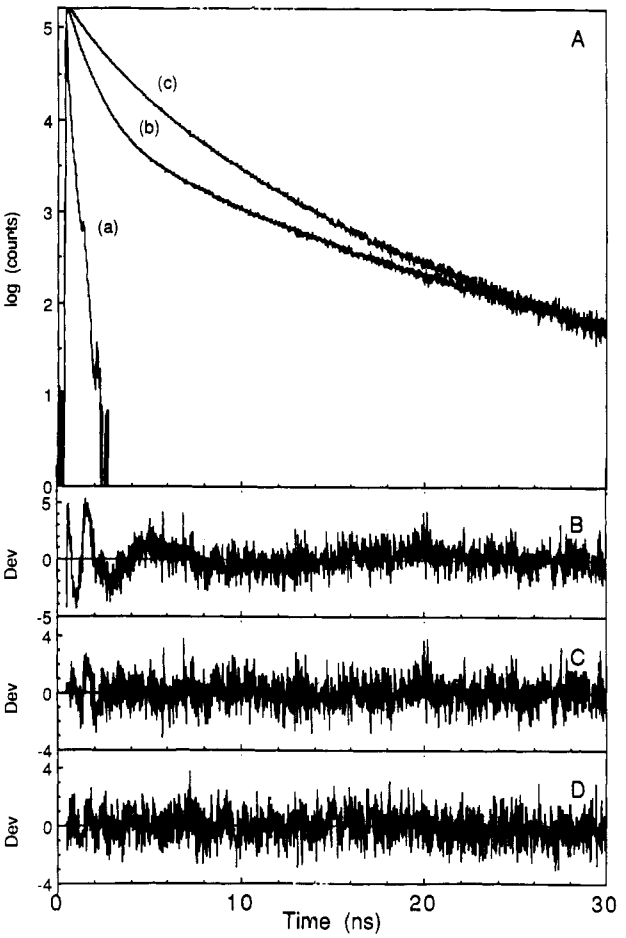

FIGURE 4: (A) Tryptophan fluorescence decays of oxidized and reduced *E. coli* thioredoxin at 20 °C, pH 7.5, λ_{exc} = 300 nm, $\lambda_{em} \geq$ 370 nm: (a) instrumental response function; (b) fluorescence decay of *E. coli* Trx-S_2; (c) fluorescence decay of *E. coli* Trx-$(SH)_2$. (B) Residuals of the least-squares fit of the fluorescence decays of Trx-S_2 to four exponential functions; the χ^2 was 1.86. (C) Residuals of the least-squares fit of the fluorescence decays of Trx-S_2 to five exponential functions. (D) Residuals of the least-squares fit of the fluorescence decays of Trx-$(SH)_2$ to four exponential functions. The corresponding parameters are given in Tables IIIA and IVA.

ascribed to the time-dependent dipolar relaxation of the protein matrix around the excited dipole of the fluorophore. In viscous media, the dipolar reorganization of the solvent may be slowed down to a time scale comparable to the decay of the fluorescence, and emission occurs in this case from different incompletely relaxed states with different intermediate spectral properties (Bakshiev, 1964; Loring et al., 1987). As would be expected from such a model, we found that the difference in lifetimes between the blue and the red edge of the thioredoxin emission decreases when the temperature increases (data not shown). In the reduced form, the different lifetime values increase also systematically with wavelength (Table IVA), but the composition of the decays also is now more clearly dependent on the wavelength, the weight of the 1-ns component increasing at the red edge of the emission, while the 0.3- and 5.0-ns components give a higher participation at the blue edge.

Some reconstructed spectra obtained by MEM analysis of the fluorescence decays at 20 °C are shown in Figures 5 and 6 for Trx-S_2 and Trx-$(SH)_2$, respectively (see also Figures 7B and 8B for $\lambda \geq 370$ nm). On the red edge of the spectrum ($\lambda \geq 370$ nm, $\lambda \geq 389$ nm), the lifetime distributions are composed of well-separated peaks. The resolution of these peaks is only slightly lower than that obtained for the MEM

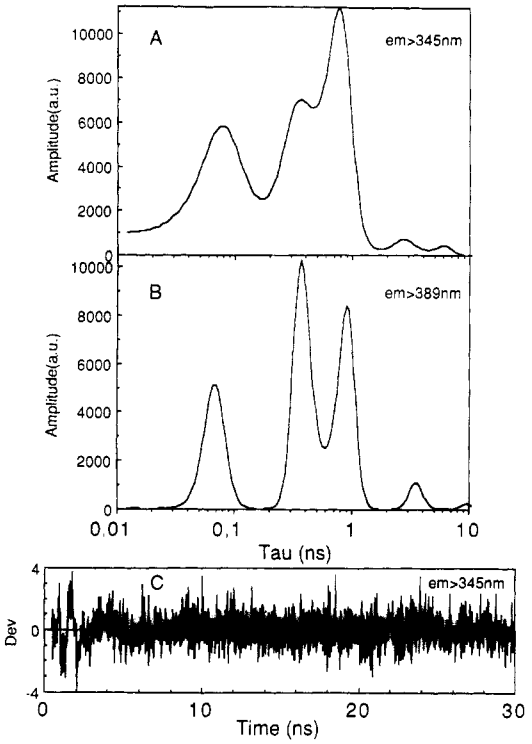

FIGURE 5: MEM reconstructed lifetime spectra of *E. coli* Trx-S_2 as a function of emission wavelength, 20 °C. (A) $\lambda_{em} \geq 345$ nm, 90 iterations performed. (B) $\lambda_{em} \geq 389$ nm, 110 iterations performed. (C) Deviation function obtained at $\lambda_{em} \geq 345$ nm. Similar residuals were obtained at the other wavelengths. The corresponding parameters are given in Table IIIB.

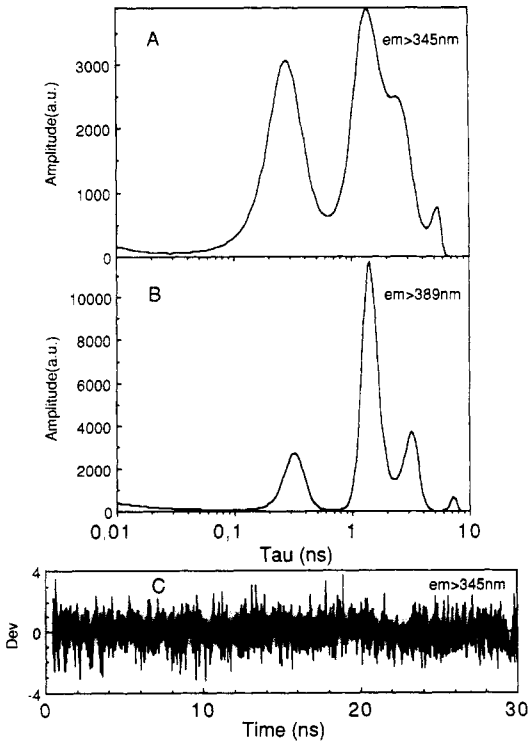

FIGURE 6: MEM reconstructed lifetime spectra of *E. coli* Trx-$(SH)_2$ as a function of emission wavelength, 20 °C. (A) $\lambda_{em} \geq 345$ nm, 50 iterations performed. (B) $\lambda_{em} \geq 389$ nm, 80 iterations performed. (C) Deviation function obtained at $\lambda_{em} \geq 345$ nm. Similar residuals were obtained at the other wavelengths. The corresponding parameters are given in Table IVB.

analysis of a synthetic discrete distribution (Figure 2A). The weight and positions of the different peaks closely correspond to the values obtained in the least-squares analysis (Tables IIIB and IVB). However, when the broader filter ($\lambda \geq 345$ nm) is used, these components broaden and merge, resulting in unresolved spectra in both oxidized and reduced thioredoxin. The different peaks separated at longer wavelengths may still be traced as the main components of these spectra and are probably well represented by the parameters obtained in the least-squares fit. This broadening is fully consistent with the solvent relaxation mechanism proposed above: since this process is expected to generate different lifetimes with different emission spectra, selecting larger emission bandwidths should result in broader lifetime distributions.

Table V: Fluorescence Decay Parameters of *E. coli* Trx-S_2 at Different Temperatures, $\lambda_{em} \geq 370$ nm

temp (°C)	lifetimes (ns) and amplitudes					mean lifetime (ns)	χ^2
	(A) Least-Squares Analysis						
−5[a]	0.08	0.34	1.28	2.96	7.8	1.08	1.06
	0.21	0.21	0.50	0.07	0.02		
5	0.08	0.37	1.03	3.00	7.7	0.77	1.13
	0.28	0.21	0.46	0.04	0.01		
20	0.07	0.34	0.86	3.18	7.8	0.51	1.14
	0.36	0.33	0.28	0.03	0.01		
30	0.07	0.31	0.84	3.16	8.0	0.38	1.17
	0.44	0.38	0.16	0.02	<0.01		
40	0.06	0.28	0.86	3.05	8.2	0.28	1.34
	0.50	0.39	0.09	0.02	<0.01		
	(B) MEM Analysis						
−5[a]	0.05	0.27	1.37		(6.09)	1.01	1.05
	0.21	0.22	0.54		(0.03)		
5	0.08	0.32	1.00	3.39	7.9	0.77	1.11
	0.28	0.15	0.52	0.03	0.01		
20	0.07	0.34	0.83	3.33	8.7	0.48	1.09
	0.38	0.30	0.29	0.02	<0.01		
30	0.06	0.31	0.80	3.15	7.7	0.36	1.13
	0.46	0.36	0.16	0.02	<0.01		
40	0.05	0.28	0.85	2.99	7.6	0.27	1.27
	0.52	0.38	0.08	0.02	<0.01		

[a] 25% glycerol.

(*d*) *Temperature Dependency of the Fluorescence Decays.* The parameters of the fluorescence decays of Trx-S_2 measured at different temperatures ($\lambda \geq 370$ nm) are given in Table V. The mean fluorescence lifetime of thioredoxin decreases with temperature, which is expected. However, the values of the different components of the decay only show a limited sensitivity to temperature, and most of the decrease in the mean lifetime is due to changes in the relative weights of these components: the contribution of the 0.9-ns longer component shifts toward the shorter 0.07- and 0.3-ns components. In the reduced form, the temperature sensitivity of the lifetime values is more marked (Table VI). However, the temperature brings also large changes in the composition of the decay, by shifts from lifetimes 3.0 and 5.0 ns toward the 1.0-ns component.

Figures 7 and 8 show the MEM spectra recovered for Trx-S_2 and Trx-$(SH)_2$ at the different temperatures for $\lambda \geq 370$ nm. While the shifts in lifetime populations upon temperature can be traced very clearly in these spectra, it can be seen also that, at 20 °C and above, the MEM spectra are composed of well-separated species, while the different lifetime components broaden at low temperatures. When going down to −5 °C in 25% glycerol for the oxidized form, this results in a "continuum" covering the entire range of lifetimes. On the other hand, the residual systematic deviation observed at short times in the fluorescence decays of Trx-S_2 disappears at low temperature, while it becomes more pronounced at high temperature (Figure 7D–F). This dependency was also observed in the least-squares analysis, while the deviation is absent from the fluorescence decays of Trx-$(SH)_2$ up to 40 °C (Figure 8D).

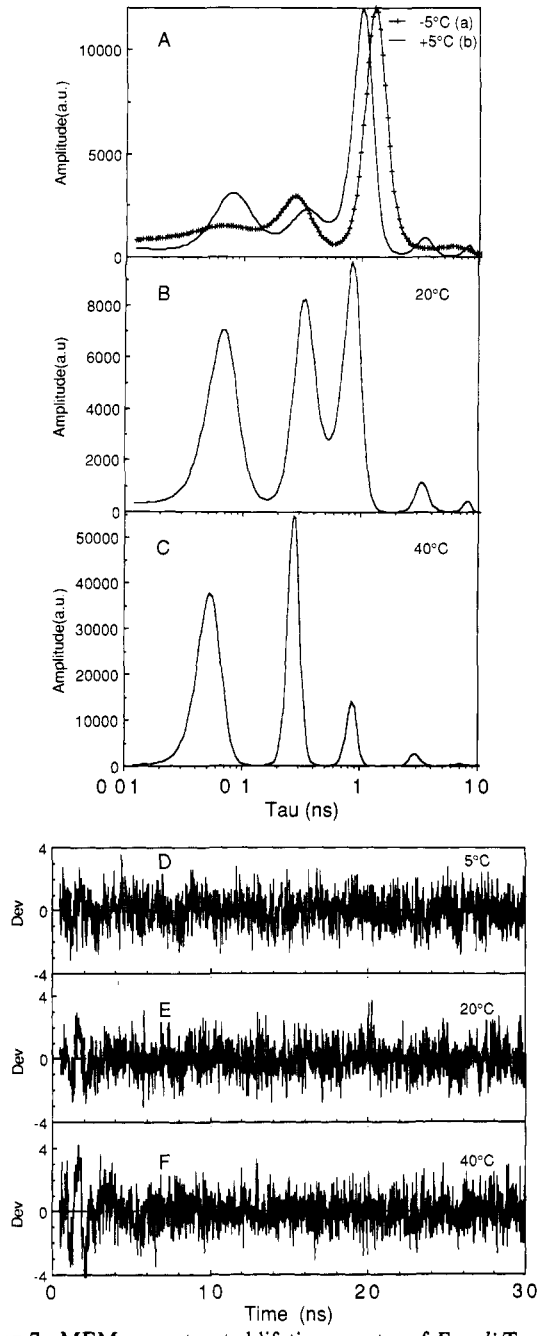

FIGURE 7: MEM reconstructed lifetime spectra of *E. coli* Trx-S_2 as a function of temperature, $\lambda_{em} \geq 370$ nm. (A) (a) −5 °C in 25% glycerol, 75% Tris buffer, 50 iterations performed; (b) +5 °C in Tris buffer, 80 iterations performed. (B) 20 °C, 110 iterations performed. (C) 40 °C, 190 iterations performed. (D–F) Deviation functions obtained at 5, 20, and 40 °C, respectively. The corresponding parameters are given in Table VB.

Therefore, it cannot be ascribed to instrumental distortions or radio-frequency pickup, but would be assigned to a fast, temperature-dependent kinetic process in the protein.

(*e*) *Fluorescence Anisotropy Decays at Room Temperature.* The correlation time for the Brownian rotation of thioredoxin approximated to a rigid sphere may be evaluated from the Einstein–Stockes relation (eq 9), assuming the specific molar volume of 0.73 mL/g for proteins and an additional "hydration" volume of 50%, which is a minimum experimental value in most proteins (Wahl, 1980). At 20 °C, the rotational correlation time of a protein of M_r 11 700 like thioredoxin would thus be around 5.3 ns.

The mean relaxation time of the fluorescence anisotropy decays of *E. coli* Trx-S_2 (Figure 9) is about 5.4 ns at 20 °C

Table VI: Fluorescence Decay Parameters of *E. coli* Trx-$(SH)_2$ at Different Temperatures, $\lambda_{em} \geq 370$ nm

temp (°C)	lifetimes (ns) and amplitudes				mean lifetime (ns)	χ^2
	(A) Least-Squares Analysis					
5	0.35	1.40	3.11	5.76	1.99	1.04
	0.32	0.26	0.34	0.08		
20	0.26	1.18	2.46	5.25	1.41	1.22
	0.30	0.39	0.27	0.04		
30	0.31	1.10	2.52	5.42	1.21	1.19
	0.30	0.51	0.18	0.02		
40	0.32	0.90	2.17	4.74	1.03	1.22
	0.28	0.52	0.18	0.02		
	(B) MEM Analysis					
5	0.39		(2.80)		1.90	1.02
	0.33		(0.66)			
20	0.27	1.26	2.56	5.43	1.40	1.09
	0.31	0.42	0.24	0.03		
30	0.32	1.13	2.57	5.58	1.20	1.15
	0.29	0.52	0.17	0.01		
40	0.33	0.92	2.25	4.92	1.02	1.09
	0.29	0.53	0.16	0.02		

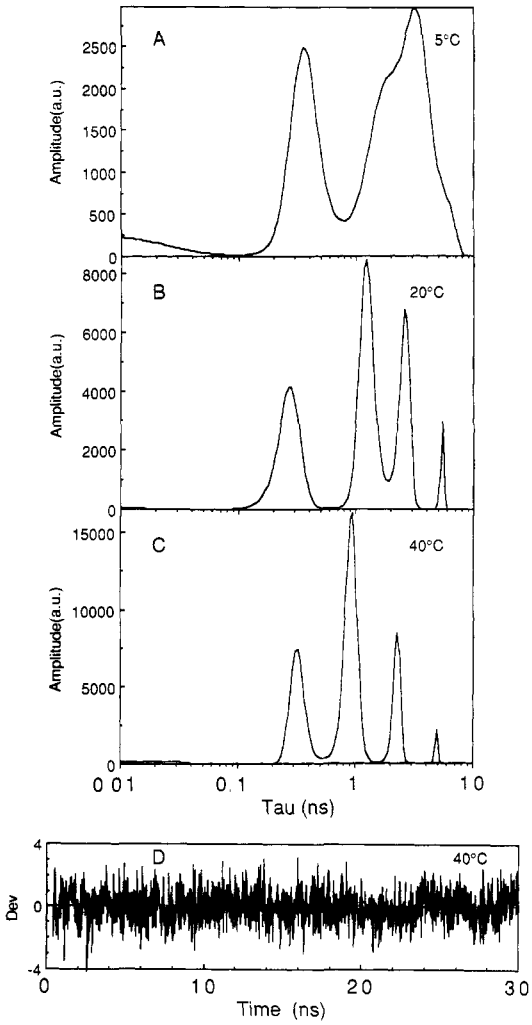

FIGURE 8: MEM reconstructed lifetime spectra of *E. coli* Trx-$(SH)_2$ as a function of temperature, $\lambda_{em} \geq 370$ nm. (A) 5 °C, 40 iterations performed. (B) 20 °C, 80 iterations performed. (C) 40 °C, 110 iterations performed. (D) Deviation function obtained at 40 °C. Similar residuals were obtained at the other temperatures. The corresponding parameters are given in Table VIB.

(Table VII). However, the decay is not correctly fitted by a single-exponential function, and two exponential terms are necessary to reach a good fit (Figure 9C,D), with a short

Table VII: Tryptophan Fluorescence Anisotropy Decays of Thioredoxins[a]

	r_0	mean θ^b (ns)	r_{0j}, θ_j (ns)			χ^2
E. coli Trx-S_2	0.299	18		0.21	0.09	1.03
25% glycerol, −5 °C				10.5 ± 2	*c*	
E. coli Trx-S_2	0.291	5.4		0.19	0.10	1.01
				2.9 ± 0.2	30 ± 14	
E. coli Trx-$(SH)_2$	0.273	6.3		0.273		1.05
				6.3 ± 0.1		
calf thymus Trx-S_2	0.259	3.5		0.19	0.07	0.96
				1.9 ± 0.1	26 ± 10	
calf thymus Trx-$(SH)_2$	0.246	4.5		0.07	0.17	1.05
				2.1 ± 0.7	6 ± 1	
yeast Trx-S_2	0.269	2.8	0.10	0.13	0.04	0.98
			0.07 ± 0.01	2.3 ± 0.2	*c*	
yeast Trx-$(SH)_2$	0.253	3.2	0.06	0.07	0.12	0.97
			0.23 ± 0.04	1.4 ± 0.4	7.4 ± 0.6	

[a] $\lambda_{em} \geq 370$ nm, 20 °C, except the glycerol experiment. [b] From analysis with a single-exponential term. [c] Nonmeasurable (uncertainty higher than the parameter value).

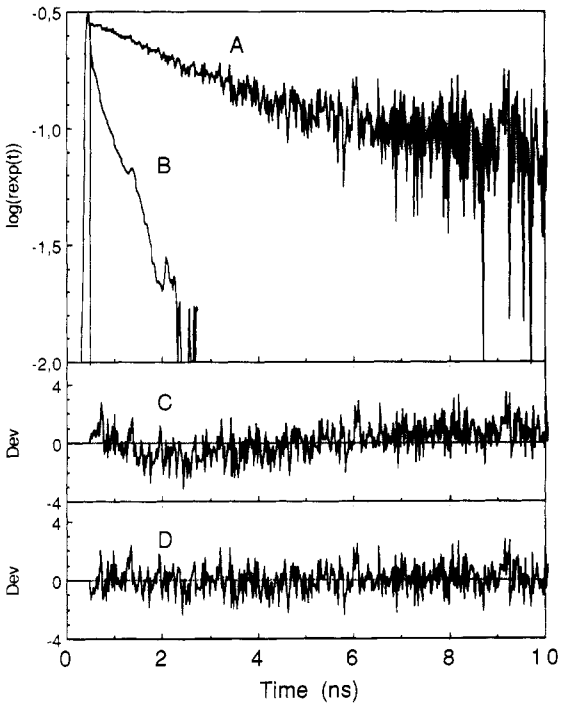

FIGURE 9: Experimental representation of the tryptophan fluorescence anisotropy decay of *E. coli* Trx-S_2 at 20 °C, pH 7.5, λ_{exc} = 300 nm, $\lambda_{em} \geq 370$ nm. (A) Experimental anisotropy decay. (B) Instrumental response. Only the least noisy part of the decay (10 ns) is shown. Analysis was performed down to 17 ns. (C) Residuals of the least-squares fit of the decay with a single-exponential term, the χ^2 was 1.55. (D) Residuals of the least-squares fit of the decay with two exponential terms. The corresponding parameters are given in Table VII.

component at 2.9 ns that accounts for two-thirds of the total amplitude and a poorly determined long component around 30 ± 14 ns (Table VII). On the other hand, the high initial anisotropy (0.29), as compared to the maximum anisotropy of tryptophan at 300 nm (0.30), shows that the fast subpicosecond flexibilities have low amplitudes.

In *E. coli* Trx-$(SH)_2$, the fluorescence anisotropy decay is well fitted by a single-exponential function, with a time constant of 6.3 ns, while the initial anisotropy r_0 is slightly but systematically lower than in the oxidized form (Table VII). Since the anisotropy decay is a simple exponential, the 6.3-ns relaxation time could represent a good approximation of the overall rotation of the protein.

The occurrence of a long, although very inaccurate, relaxation time around 30 ns in the anisotropy decay of Trx-S_2 may suggest some aggregation. Association of thioredoxin into dimers was observed at acidic pHs (Holmgren, 1985). However, we did not observe any significant change in the measured correlation time of thioredoxin over the concentration range 85–940 μM (lower protein concentrations were not possible because of the low quantum yield of thioredoxin). Moreover, no evidence for aggregation was found in NMR experiments done on both oxidized and reduced thioredoxin at a 4 mM protein concentration. On the other hand, the rotational relaxation time obtained for the reduced protein is an acceptable value for the overall rotation of monomeric thioredoxin, while the reduced form is known to have a higher tendency to aggregate.

(f) Fluorescence Anisotropy Decay at Low Temperature in 25% Glycerol. Some excitation energy transfers could occur between the two tryptophan residues of *E. coli* thioredoxin and induce time-dependent depolarizations of the fluorescence that would have to be separated from the true rotational dynamics of the protein. Although the excitation wavelength at 300 nm, on the red edge of the tryptophan absorption spectrum, is likely to minimize the amplitude of such processes (Weber & Shinitzki, 1970), we checked for these depolarizations by measuring the fluorescence anisotropy decays of the oxidized protein immobilized in a 25% glycerol mixture at −5 °C.

The anisotropy decay obtained in these conditions shows the same overall composition as at 20 °C, except that the time constants are longer (Table VII). The longest component of the decay is too slow to be measured, but a shorter component of 10.5 ns can be separated. The hypothesis that this component precisely corresponds to energy transfers cannot be excluded, but it seems more likely, given its high amplitude and the general composition of the decay, that this component is related to remaining slow flexibilities in the structure. The viscosity of a 25% glycerol mixture at −5 °C is approximately 5 cp, which gives a η/T ratio of 18.7×10^{-3} cP/K, while the η/T ratio in water at 20 °C is 3.43×10^{-3} cP/K. As estimated from eq 9, the 2.9-ns component at 20 °C should thus increase to 16 ns in the glycerol mixture at −5 °C. Therefore, the experiment may not have allowed a complete blocking of all flexibilities in the protein.

Besides this component, no other fast depolarization process is found, and the initial anisotropy is close to the 0.30 maximal value expected for tryptophan at an excitation wavelength of 300 nm (Valeur & Weber, 1977). Therefore, it is unlikely that the fast depolarizations found in *E. coli* Trx-S_2 at room temperature are due to energy transfers.

Calf Thymus Thioredoxin. The fluorescence quantum yield of calf thymus Trx-S_2 approximately equals that of *E. coli*

Table VIII: Fluorescence Decay Parameters of Calf Thymus Thioredoxin at $\lambda_{em} \geq 370$ nm, 20 °C

oxidation state	lifetimes (ns) and amplitudes					mean lifetime (ns)	χ^2
	(A) Least-Squares Analysis						
Trx-S_2	0.05	0.35	0.94	3.58	8.7	0.71	1.11
	0.38	0.30	0.24	0.07	0.01		
Trx-$(SH)_2$	0.06	0.28	1.36	3.11	8.1	1.04	1.03
	0.24	0.31	0.30	0.14	0.01		
	(B) MEM Analysis						
Trx-S_2	0.05	0.33	0.86	(4.05)		0.66	1.04
	0.41	0.25	0.26	(0.08)			
Trx-$(SH)_2$	0.05	0.26		(2.06)		0.99	1.11
	0.24	0.32		(0.43)			

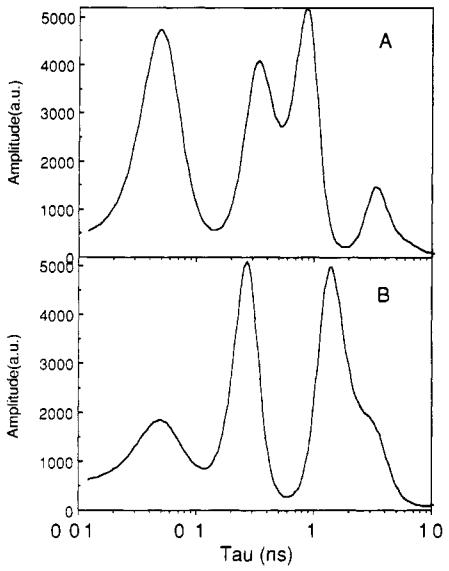

FIGURE 10: MEM reconstructed lifetime spectra of calf thymus Trx-S_2 and Trx-$(SH)_2$ at 20 °C, $\lambda_{em} \geq 370$ nm. (A) Calf thymus Trx-S_2, 70 iterations performed. (B) Calf thymus Trx-$(SH)_2$, 100 iterations performed. The corresponding parameters are given in Table VIII.

thioredoxin (Table II). However, reduction brings only a 1.5-fold increase in the overall quantum yield, paralleled by an equal increase in mean lifetime, while the overall shape of the steady-state fluorescence spectrum does not change markedly. The level of static quenching is higher than in the *E. coli* protein and remains constant upon reduction (Table II).

Although calf thymus thioredoxin contains only one tryptophan residue, the fluorescence decays are almost as complex as those of *E. coli* thioredoxin, with five exponential components separated in the least-squares analysis of both oxidized and reduced forms. The fluorescence compositions (Table VIII) are roughly comparable to those observed for the *E. coli* protein, with very similar values of the different lifetimes. The MEM spectra (Figure 10) show a lower resolution as compared to *E. coli* thioredoxin, which may be ascribed to the necessary subtraction of a blank, and therefore the lower statistical accuracy of the data. No apparent structure was observed in the deviation functions (data not shown), which may be also a consequence of the blank subtraction. As in the *E. coli* protein, reduction decreases the weight of the shortest 0.05-ns component of the decay, to the benefit of the 3-ns component, but a significant percentage of this short component is still observed in the reduced form. The reduction process may, however, be somewhat different in the case of calf thymus thioredoxin since this protein contains an extra structural disulfide bridge that may compete with the functional one for the global reducing power (Holmgren, 1985).

Table IX: Fluorescence Decay Parameters of Yeast Thioredoxin at $\lambda_{em} \geq 370$ nm, 20 °C

oxidation state	lifetimes (ns) and amplitudes					mean lifetime (ns)	χ^2
	(A) Least-Squares Analysis						
Trx-S_2	0.03	0.25	1.36	2.41	8.9	0.34	1.11
	0.73	0.09	0.13	0.04	<0.01		
Trx-$(SH)_2$	0.07	0.19	1.11	3.54	7.0	0.56	1.17
	0.51	0.34	0.06	0.09	0.01		
	(B) MEM Analysis						
Trx-S_2	0.03	0.27		(1.65)		0.33	1.07
	0.75	0.08		(0.16)			
Trx-$(SH)_2$	0.07	0.18	1.11	3.62	7.2	0.54	1.08
	0.55	0.30	0.05	0.09	0.01		

The fluorescence anisotropy decays of oxidized and reduced calf thymus thioredoxin are faster than those of the *E. coli* protein, as seen from their mean relaxation times (Table VII). However, the overall composition of the decay in the oxidized form is very similar, including a short component faster than the overall rotation of the protein and a long, poorly determined component. As in the *E. coli* protein, reduction brings an increase in the mean relaxation time of the decay and a slight decrease in the initial anisotropy. However, the short component is still present in the reduced form of calf thymus thioredoxin. This may be related to the possible incomplete reduction of the protein, as already suggested by the fluorescence decays, or to remaining internal flexibilities of the tryptophan residue. The long component of the anisotropy decay of calf thymus Trx-$(SH)_2$, which in simplified models would correspond to the overall rotation of the protein (M_r 12000), is close to that measured on *E. coli* Trx-$(SH)_2$, which is expected for these two proteins of very similar size.

Yeast Thioredoxin. The steady-state fluorescence intensity of the single tryptophan residue in yeast thioredoxin is extremely weak, with an approximate quantum yield of only 0.7% in the oxidized form (Table II). Even with an excitation at 300 nm, an important tyrosin contribution can be seen on the blue edge of the fluorescence spectra, resulting in a large FWHM. We found a 1.7-fold increase in the fluorescence quantum yield of yeast thioredoxin upon reduction, which is higher than what was previously observed (Holmgren, 1972). In this latter study, the fluorescence spectra were recorded with an excitation at 280 nm and contained a high contribution of tyrosyl fluorescence, which may have damped the tryptophan response. As in the calf thymus protein, the level of static quenching in yeast thioredoxin is higher than for the *E. coli* protein and approximately constant between the oxidized and reduced forms (Table II).

Although it was possible to fit, by a least-squares procedure, the fluorescence decays of the single tryptophan residue of yeast Trx-S_2 with up to five exponential components (Table IXA), the MEM analysis of the same data (Table IXB and Figure 11A) shows that there is definite evidence for at most four of them: three major components are centered respectively at 0.03, 0.26, and 1.64 ns, while a fourth one with very low weight is badly separated from the 1.64-ns component (therefore, the value of this third component is overestimated). No apparent structure was observed in the deviation functions (data not shown). Because of the subtraction of a blank, the data for the yeast protein are of lower statistical accuracy than for the *E. coli* and calf thymus proteins, and some components with low relative weight may have escaped detection. Nevertheless, a very short lifetime at the limit of the instrumental resolution is now almost completely dominating the emission

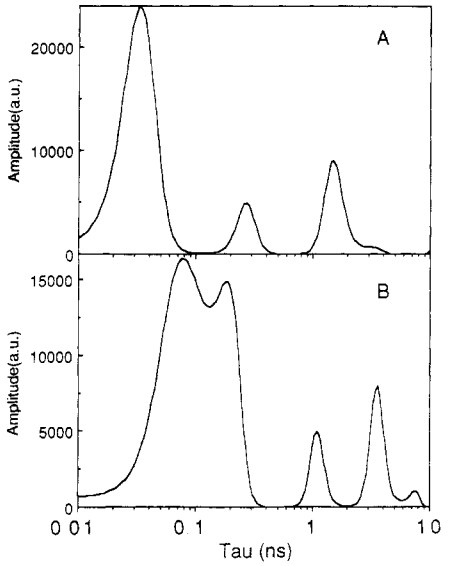

FIGURE 11: MEM reconstructed lifetime spectra of yeast Trx-S_2 and Trx-$(SH)_2$ at 20 °C, $\lambda_{em} \geq 370$ nm. (A) Yeast Trx-S_2, 110 iterations performed. (B) Yeast Trx-$(SH)_2$, 130 iterations performed. The corresponding parameters are given in Table IX.

of the oxidized form. Reduction results mainly in exchanges between very short lifetime components (Figure 11B), and therefore the spectroscopic events associated with the reduction of yeast thioredoxin appear rather different from those occurring in the calf thymus and *E. coli* proteins. Given the excitation wavelength and the emission bandwidth used in these experiments ($\lambda \geq 370$ nm), it is, however, unlikely that this discrepancy arises from a significant participation of the tyrosyl emission in the fluorescence decays (Lakowicz, 1983). On the other hand, a very careful control of the buffer was performed in view of the blank subtraction (see Experimental Procedures), and it is therefore also excluded that such large differences are due to some fluorescent contaminants in the samples.

The yeast protein shows complex fluorescence anisotropy decays that cannot be fitted by less than three exponential functions in both oxidized and reduced forms (Table VII). This, together with the low value of the mean relaxation time, suggests a high degree of flexibility of the single tryptophan residue in this protein. The long component is not measurable in the oxidized form, due to its low associated amplitude together with the extremely short fluorescence-carrying signal of yeast thioredoxin. However, similarly to the other thioredoxins, reduction brings a significant increase in the amplitude of this long component, as well as a decrease in the initial anisotropy.

Discussion

Steady-State Tryptophan Fluorescence of Thioredoxin. Early studies have shown that disulfides and sulfhydryl groups (Cowgill, 1967) as well as cysteine residues (Steiner & Kirby, 1969) are strong quenchers of indole fluorescence. Since both tryptophan residues of *E. coli* thioredoxin are located very close to the active cysteines, interactions with these residues are likely to account for most of the strong observed quenching, although other interactions with neighboring polar groups (Asp-26, Glu-30, Lys-36), with the peptide bond, or between the two tryptophan residues themselves should not be a priori excluded.

We found that this quenching results from both collisional interactions (dynamic quenching) and formation of a nonfluorescent complex on the ground state (static quenching). The chemical groups responsible for these different quenchings could be identical if stable, short-range interactions are allowed between the fluorophore and a high local concentration of quencher (Lakowicz, 1983). From NMR and CD studies (Lebl et al., 1987; Bodner et al., 1980) as well as in the crystal structure of proteins (Morgan et al., 1978; Morgan & McAdon, 1980), there are numerous indications of stable, noncovalent interactions of sulfur or disulfides with aromatic compounds. In several fluorescence studies (Cowgill, 1967; Steiner & Kirby, 1969; Swadesh et al., 1987; Roy & Mukherjee, 1987; Ross et al., 1986), the quenching of tyrosyl or indole fluorescence by sulfur-containing compounds has been shown to result in large part from static interactions. For example, the Tyr residue adjacent to the disulfide bridge of oxytocin exhibits 38% static quenching (Ross et al., 1986). Replacement of the disulfide by an ethylene bridge leads to a complete suppression of this static quenching.

In keeping with the previous fluorescence studies, we observe in all native thioredoxins an increase in fluorescence quantum yield and mean lifetime upon reduction. A 1.2-fold increase in the fluorescence of bis(indole-3-methyl) disulfide upon reduction was observed by Cowgill (1967). A 1.3-fold increase in fluorescence intensity was also reported for the reduction of oligopeptides modeling the active disulfide loop of thioredoxin, such as Boc-Trp-Cys-Gly-Pro-Cys-NHMe (Kishore et al., 1983). The fluorescence signal of the tyrosine residues of glutaredoxin (Höög et al., 1983) and T4 thioredoxin (Berglund & Holmgren, 1975) were also reported to increase upon reduction. These systematic increases probably reflect the relative quenching ability of the disulfide bridge and the sulfhydryl groups: the oxidized disulfide bridge is a better electron acceptor than the reduced sulfhydryl group, and, under an electron-transfer model (see below), would thus induce a faster quenching of tryptophan fluorescence. The increases in fluorescence intensity of the yeast and calf thymus proteins could be accounted for in large part by this simple dielectric effect.

Steiner and Kirby (1969) have proposed that cysteine mainly acts as an electron scavenger in the quenching of indole fluorescence. Roy and Mukherjee (1987) also concluded in favor of a charge-transfer mechanism in the quenching of indole by ethylene trithiocarbonate. Moreover, in the study of a large set of tryptophan analogues, Petrich et al. (1983) showed that a dominant nonradiative deexcitation pathway for tryptophan was electron transfer to a neighboring acceptor or from a donor (Miller et al., 1982), possibly enhanced in some cases by delocalizing interactions. The stabilization of a charge-transfer complex between tryptophan and cystine could provide an optimized pathway for reductive electron transfer in the protein and may be one of the interactions responsible for the exceptional reactivity of the thioredoxin disulfide (Holmgren, 1985).

Time-Resolved Tryptophan Fluorescence of Thioredoxin. (*a*) *Very Fast Fluorescence Kinetics.* A high proportion of a very short fluorescence component is found in all oxidized thioredoxins studied here. It is mainly characteristic of the oxidized state of the protein, since a decrease or even a complete suppression of this component occurs upon reduction of all proteins. The short component is not observed up to 40 °C in *E. coli* Trx-$(SH)_2$. This component is also absent from all aqueous tryptophan derivatives studied so far (Petrich et al., 1983) and thus may be specifically related to the electron-transfer mechanism mentioned above.

On the other hand, at room temperature and above, the fluorescence decays of *E. coli* Trx-S_2 cannot be fitted properly

at very short times, and this residual distortion shows temperature dependency. This is observed also in the MEM analysis, even though in this case a large set of short lifetime values is available for the fit of complex decay kinetics. Therefore, it must be concluded that the fluorescence decays at these short times are not correctly represented by sums of positive exponential functions. Negative exponential terms may arise from the buildup, from the initially excited state, of a new population of emitting species, which could be due to successive steps in the slow protein matrix dielectric relaxation. On the other hand, in the simplest models of collisional quenching in a bulk solvent (Smoluchowski, 1917), the fluorescence decay is predicted to depart from a simple exponential behavior at short times and to follow approximately a law of the form $\exp(-at - bt^{1/2})$. In the case of collisional quenching in a protein matrix, all approximations relative to the bulk properties of the solvent should be reconsidered, which may lead to rather more complex kinetic laws at short times. No attempt was made for the moment to fit the thioredoxin data with any of the available models. It should be noted, however, that the short-lifetime component may be affected by this uncorrect description of the data at short times.

(*b*) *Evidence for Discrete Species.* In the least-squares analysis, the fluorescence decays of the two tryptophan residues of *E. coli* Trx-S_2 need five exponential components to be described. Moreover, calf thymus and yeast thioredoxins, which contain only one tryptophan residue, exhibit at least four exponential decays. These results range among the most complex reported today in pulse fluorometry studies of single or multiple tryptophan containing proteins, where a maximum of three to four components is usually separated (Beechem & Brand, 1985; Ludescher et al., 1985; Vincent et al., 1988). This may be ascribed to the peculiar fluorescence properties of thioredoxin, but reflects also the high resolution of the data collected. As the temporal resolution of pulse fluorometry measurements improves, the fluorescence properties of proteins appear increasingly complex. Meanwhile, recent theoretical and experimental works have put the emphasis on the multiplicity of conformational "substates" in proteins (Elber & Karplus, 1987; Ansari et al., 1987). Therefore, many authors suspect today that the protein fluorescence might be better described in terms of continuous distributions of lifetimes (Ludescher et al., 1985; James & Ware, 1985; Alcala et al., 1987). In this view, the discrete compositions obtained through a least-squares fit of the data might be an arbitrary representation without physical meaning (James & Ware, 1985). However, when large smooth distributions of lifetimes are "overfitted" by a small set of discrete components, the number, position, and relative weight of these components are highly dependent on the sample of random noise added to the simulations (Mérola et al., unpublished results). On the contrary, the stability of the thioredoxin lifetimes throughout the different experiments suggests that a discrete representation of the data may be meaningful in this case. The MEM analysis brings further strong support to this idea.

Several methods have been recently developed for the recovery of lifetime distributions (James & Ware, 1986; Alcala et al., 1987; Lakowicz et al., 1987; Philipps & Lyke, 1987). Most of them make use of analytical models for the lifetime distribution $A(\tau)$ or otherwise remain limited to the fit of a small number of decay times. The maximum entropy method allows a large set of lifetimes to be handled, with much fewer a priori assumptions (although models can also be encoded in the analysis). The present simulations, after those of Livesey et al. (Livesey et al., 1986, 1987; Livesey & Brochon, 1987) and Vincent et al. (1988), demonstrate the ability of the MEM analysis to discriminate between continuous and discrete models in data of sufficient statistical accuracy. Indeed, we found some experimental examples of both types of distributions. However, due to the degeneracy of the problem of Laplace transform, the MEM analysis should not be expected to provide unambiguously the "right" image in the frequency domain of noisy fluorescence decays. In this view, the simulations presented here may give some insight to the "feasible set" within which were chosen our "preferred" solutions (Livesey & Brochon, 1987). Moreover, they show that the spectra obtained for thioredoxin at room temperature and for narrow emission bandwidth are compatible only with the simulations based on highly resoluted discrete components.

It should be stressed that, contrary to the steady-state NMR situation, large distributions of lifetimes cannot merely result from two or more discrete fluorescent components exchanging on the time scale of the excited state: the kinetic description of such a system predicts only as many discrete exponential terms as initially exchanging components, while the lifetimes will reduce to a single average value in the case of a fast exchange (Donzel et al., 1974). Only when a continuum of excited states preexists, or if the interconversion rates are themselves continuously distributed, and provided that these distributions are not averaged by fast exchanges, may it produce fluorescence lifetime distributions. For two fluorescence lifetimes differing by a factor of 3, averaging will occur approximately for exchange times equal to half the shortest lifetime (Engh et al., 1986). Although distributions of energy substates may widely occur in proteins, it seems that, in the case of thioredoxin at room temperature, the fast exchanges are sufficient to average most of these distributions. Nevertheless, the fluorescence appears to be composed of several discrete emitting species that behave relatively independently. It may well be, however, that in the case of other proteins, containing, for example, strongly immobilized tryptophan residues, continuous distributions of lifetimes will be observed in the same conditions. General statements will be possible only when a large set of highly resoluted data will be available and analyzed with the minimum a priori assumptions: precisely because of the ill-conditioned nature of the Laplace transform, illegitimate constraints imposed on the analysis are expected to meet only weak denial from the data.

(*c*) *Large Distributions Observed in Temperature and Wavelength Studies.* At low temperature and with large detection bandwidth, we found some examples of broad lifetime distributions. The broadening of the MEM spectra when a large set of emission wavelengths is simultaneously detected is well accounted for by a time-dependent relaxation of the protein matrix, and of the emitting energy level, after excitation. Similarly, the broadening of the distributions at low temperatures might be linked to the further slow down of this matrix relaxation, as well as of all other rates of exchanges responsible for averaging at room temperature. A similar broadening of the fluorescence lifetime distribution of denatured apomyoglobin at low temperature has been reported by Bismuto et al. (1988). However, the lifetime spectra of thioredoxin at low temperature do not show evidence for new discrete species or marked changes in the lifetime values, as would be expected if two largely differing components were merged by fast exchange at room temperature [although the lifetimes of Trx-$(SH)_2$ show a somewhat higher sensitivity to temperature]. Therefore, it must be concluded that the possible exchanges between these lifetimes are either too fast or

too slow to be significantly temperature dependent on the nanosecond time scale. In other words, the discrete lifetime values observed at room temperature are unlikely to be spurious averages of species with very different fluorescence kinetics and mean dynamic interactions, but rather some barycenters of closely related conformers. As a result, the changes in the thioredoxin lifetime spectra, over the temperature range studied, are mainly governed by the temperature dependency of equilibrium constants between the different discrete species. This would imply that there is a large gap on the nanosecond time scale in the dynamics of the tryptophan residues. Strikingly, some recent long-range (600 ps) molecular dynamics simulations of tryptophans in myoglobin (Henry & Hochstrasser, 1987) have come to a very similar picture, where the tryptophan side chains would experience both small rapid reorientational fluctuations and large infrequent transitions between conformers related by 120° rotations. This description would not depart very much also from the rotamer model proposed earlier to account for the multiexponential decay of aqueous tryptophan (Szabo & Rayner, 1980; Engh et al., 1986). If the different rotamers of tryptophan around a single C–C bond in water do not exchange rapidly on the nanosecond time scale, they can also be expected to exchange slowly in a protein matrix. In this latter case, the heterogeneity of the fluorescence may result from the combination of both the tryptophan side chain and the protein matrix conformers.

Fluorescence Anisotropy Decays of Thioredoxin. The nonexponential fluorescence anisotropy decay of *E. coli* Trx-S_2, with a high initial anisotropy and without any fast subnanosecond component, suggests that the tryptophan residues of the protein have some limited flexibilities in an otherwise relatively rigid structure. The fast averaging exchanges assumed to account for the observed discrete species in the fluorescence decays do not induce a fast depolarization of this fluorescence and, therefore, must be of low amplitude, which would be consistent with the above proposal that these exchanges occur only between closely related conformers. On the other hand, the calf thymus and yeast proteins show faster anisotropy decays in both their oxidized and reduced forms, as compared to the *E. coli* protein, indicating that the single tryptophan residue of these proteins experiences a higher degree of mobility.

However, reduction brings several similar changes in the anisotropy decays of these different proteins. In all cases, a small decrease in the initial anisotropy r_0 shows that the breakage of the disulfide link allows a higher rate of the very fast rotations. Nevertheless, as seen from their mean relaxation times, all reduced thioredoxins show a slower decay of the fluorescence anisotropy, suggesting that, on the nanosecond time scale, some rotational freedom has been lost upon reduction. In *E. coli* thioredoxin, this results in an apparent complete blocking of the tryptophan motion on this time scale.

However, if the different fluorescence lifetimes of the protein are associated with specific rotational relaxations, the anisotropy function $r(t)$ cannot be factored out in eq 13, and each individual rotational species must be treated as a separate weighted term (Rigler & Ehrenberg, 1976; Claesens & Rigler, 1986; Ludescher et al., 1987). Calculating the anisotropy function in the classical way will result in improper normalization of each $D_k(t)$ by a global Im(t) function not related to the kth rotational specy (eq 11). Derivation of eq 12 gives

$$d\theta_k = -(\theta_k/\tau_k)^2\, d\tau_k \qquad (22)$$

which shows that, if the ratio of the rotational relaxation time to the fluorescence lifetime is high (which could be the case for the short-lived components of oxidized thioredoxin), small errors in the assumed lifetime value will result in large errors in the calculated rotational relaxation time. Ludescher et al. (1987) presented a large set of simulations showing the variety of anisotropy decay laws resulting from associated dynamics and gave some examples of the large errors brought by a classical analysis of such decays. Associated dynamics may probably account for the unphysical long decay time in the anisotropy decays of *E. coli* Trx-S_2 and may also have resulted in a spurious value of the short component. However, the nonexponentiality of the anisotropy decay definitely shows that some reorientation of the tryptophan side chain occurs in addition to the overall tumbling of the protein. The question remains open about its true time scale. In Trx-$(SH)_2$, our present interpretation would remain valid only if the observed fluorescence anisotropy decay includes the final slope of the relaxation (Ludescher et al., 1987). Since a similar long relaxation time is found as well for the single-tryptophan-containing calf thymus thioredoxin, this complex rotational behavior would not be simply linked to differences in the motion of two distinct tryptophan residues but rather to discrete dynamical states of single residues. Ludescher et al. (1987) have already pointed out that, since the different fluorescence lifetimes arise from different interactions of the fluorophore with its surrounding, it is very likely that each of these species is also associated with a specific dynamical behavior. It is striking to note that *E. coli* and calf thymus share simultaneously similar fluorescence kinetics and anisotropy decays, while the yeast protein clearly differs in both. Therefore, as soon as the fluorescence of a given system is shown to be heterogeneous (which is by far the general case for proteins), the question should be asked about the possibility of associated heterogeneity in the dynamics. Analytical degeneracy (different types of associations can result in exactly identical analytical functions) will combine here with the persistent ill conditioning of Laplace transform and the poor statistical accuracy of the data available today to make this problem an extremely difficult one to resolve. The maximum entropy method applied to the analysis of the transient polarized components of the fluorescence may help in approaching the solution of this problem with a minimum of a priori assumptions (Brochon & Livesey, 1988).

Acknowledgments

We thank A. K. Livesey for continued interest in this work and for his suggestions on the simulations and M. Vincent and J. Gallay for stimulating discussions. We also thank the technical staffs of the Medical Biophysics and Physiological Chemistry Departments at the Karolinska Institutet for skillful assistance in sample preparations and laser maintenance. Data analysis and simulations were performed on the VAX 780 computer of the crystallography department of the LURE laboratory.

Supplementary Material Available

Tabulation of quantitative parameters (average positions, fractional areas, and χ^2s) describing the initial simulations and recovered spectra of Figures 2A–C and 3A–C (6 pages). Ordering information is given on any current masthead page.

References

Alcala, J. R., Gratton, E., & Prendergast, F. G. (1987) *Biophys. J. 51*, 587–596, 597–604, 925–936.

Ansari, A., Berendzen, J., Braunstein, D., Cowen, B. R., Frauenfelder, H., Hong, M. K., Iben, I. E. T., Johnson, J. B., Ormos, P., Sauke, T. B., Scholl, R., Schulte, A., Steinbach, P. J., Vittitow, J., & Young, R. D. (1987)

Biophys. Chem. 26, 337–355.
Bakhshiev, N. G. (1964) *Opt. Spectrosc. 16*, 446–451.
Beechem, J. M., & Brand, L. (1985) *Annu. Rev. Biochem. 54*, 43–71.
Berglund, O., & Holmgren, A. (1975) *J. Biol. Chem. 250*, 2778–2782.
Bismuto, E., Gratton, E., & Irace, G. (1988) *Biochemistry 27*, 2132–2136.
Bodner, B. L., Jackman, L. M., & Morgan, R. S. (1980) *Biochem. Biophys. Res. Commun. 94*, 807–813.
Brochon, J. C., & Livesey, A. K. (1988) in *Light in Biology and Medicine* (Douglas, R. H., & Moan, J., Eds.) Vol. 1, pp 21–29, Plenum Publishing, London.
Burstein, E. A., Vedenkina, N. S., &Ivkova, M. N. (1973) *Photochem. Photobiol. 18*, 263–279.
Claesens, F., & Rigler, R. (1986) *Eur. Biophys. J. 13*, 331–342.
Cowgill, R. W. (1967) *Biochim. Biophys. Acta 140*, 37–44.
Donzel, B., Gauduchon, P., & Wahl, P. (1974) *J. Am. Chem. Soc. 96*, 801–808.
Dyson, H. J., Holmgren, A., & Wright, P. E. (1988) *FEBS Lett. 228*, 254–258.
Ehrenberg, M., & Rigler, R. (1972) *Chem. Phys. Lett. 14*, 539–544.
Elber, R., & Karplus, M. (1987) *Science 235*, 318–321.
Engh, R. A., Chen, L. X. Q., & Fleming, G. R. (1986) *Chem. Phys. Lett. 126*, 365–372.
Engström, N. E., Holmgren, A., Larsson, A., & Söderhall, S. (1974) *J. Biol. Chem. 249*, 205–210.
Gadal, P., Ed. (1983) *Thioredoxines: Struct. Fonct. Colloq. Int. CNRS-NASA 1981*, 1–288.
Gleason, F., & Holmgren, A. (1988) *FEMS Microbiol. Rev.* (in press).
Gonzales Porqué, P., Baldesten, A., & Reichard, P. (1970) *J. Biol. Chem. 245*, 2363–2370.
Gratton, E., & Lakowicz, J. R. (1985) in *Structure and motion: membranes, nucleic acids and proteins* (Clementi, E., Corongiu, G., Sarma, M. H., & Sarma, R. H., Eds.) pp 155–168, Adenine Press, Guilderland, NY.
Grinvald, A., & Steinberg, I. Z. (1974) *Anal. Biochem. 59*, 583–598.
Gull, S. F., & Skilling, J. (1984a) Maximum entropy method in image processing, *Proc. IEEE 131F*, 646–661.
Gull, S. F., & Skilling, J. (1984b) in *Indirect imaging* (Roberts, J. A., Ed.) pp 267–279, Cambridge University Press, Cambridge, U.K.
Hall, D. E., Baldesten, A., Holmgren, A., & Reichards, P. (1971) *Eur. J. Biochem. 23*, 328–335.
Henry, E. R., & Hochstrasser, R. M. (1987) *Proc. Natl. Acad. Sci. U.S.A. 84*, 6142–6146.
Holmgren, A. (1968) *Eur. J. Biochem. 6*, 475–484.
Holmgren, A. (1972) *J. Biol. Chem. 247*, 1992–1998.
Holmgren, A. (1973) *J. Biol. Chem. 248*, 4106–4111.
Holmgren, A. (1981) *Biochemistry 20*, 3204–3207.
Holmgren, A. (1985) *Annu. Rev. Biochem. 54*, 237–271.
Holmgren, A., & Reichard, P. (1967) *Eur. J. Biochem. 2*, 187–196.
Holmgren, A., & Roberts, G. (1976) *FEBS Lett. 71*, 261–265.
Holmgren, A., Soderberg, B. O., Eklund, H., & Branden, C. I. (1975) *Proc. Natl. Acad. Sci. U.S.A. 72*, 2305–2309.
Holmgren, A., Branden, C. I., Jornvall, H., & Sjoberg, B. M., Eds. (1986) in *Thioredoxin and Glutaredoxin systems: structure and function*, Raven Press, New York.
Holmgren, A., Palmberg, C., Jörnvall, H., & Hernberg, L. (1989) *J. Biol. Chem.* (submitted for publication).
Höög, J. O., Jörnvall, H., Holmgren, A., Carlquist, M., & Persson, M. (1983) *Eur. J. Biochem. 136*, 223–232.
Iyer, K. S., & Klee, W. A. (1973) *J. Biol. Chem. 248*, 707–710.
James, D. R., & Ware, W. R. (1985) *Chem. Phys. Lett. 120*, 455–459.
James, D. R., & Ware, W. R. (1986) *Chem. Phys. Lett. 126*, 7–11.
Jaynes, E. T. (1983) in *Collected Works. Papers on Probability Statistics and Statistical Physics* (Rosenkrantz, R. D., Ed.) D. Reidel, Dordrecht, Holland.
Kishore, R., Mathew, M. K., & Balaram, P. (1983) *FEBS Lett. 159*, 221–224.
Lakowicz, J. R. (1983) in *Principles of fluorescence spectroscopy*, Plenum Press, New York.
Lakowickz, J. R., & Cherek, H. (1980) *J. Biol. Chem. 255*, 831–834.
Lakowicz, J. R., Cherek, H., Gryczynski, I., Joshi, N., & Johnson, M. L. (1987) *Biophys. Chem. 28*, 35–50.
Lebl, M., Sugg, E. E., & Hruby, V. J. (1987) *Int. J. Pept. Protein Res. 29*, 40–45.
Livesey, A. K., & Brochon, J. C. (1987) *Biophys. J. 52*, 693–706.
Livesey, A. K., Licinio, P., & Delaye, M. (1986) *J. Chem. Phys. 84*, 5102–5107.
Livesey, A. K., Delaye, M., Licinio, P., & Brochon, J. C. (1987) *Faraday Discuss. Chem. Soc. 83*, paper 14.
Loring, R. F., Yan, Y. Y., & Mukamel, S. (1987) *Chem. Phys. Lett. 135*, 23–29.
Ludescher, R. D., Volwerk, J. J., de Haas, G. H., & Hudson, B. S. (1985) *Biochemistry 24*, 7240–7249.
Ludescher, R. D., Peting, L., Hudson, S., & Hudson, B. (1987) *Biophys. Chem. 28*, 59–75.
Miller, J. R., Peeples, J. A., Schmitt, M. J., & Closs, G. L. (1982) *J. Am. Chem. Soc. 104*, 6488–6493.
Morgan, R. S., & McAdon, J. M. (1980) *Int. J. Pept. Protein Res. 15*, 177–180.
Morgan, R. S., Tatsch, C. E., Gushard, R. H., McAdon, J. M., & Warme, P. K. (1978) *Int. J. Pept. Protein Res. 11*, 209–217.
Petrich, J. W., Chang, M. C., McDonald, D. B., & Fleming, G. R. (1983) *J. Am. Chem. Soc. 105*, 3824–3832.
Philipps, S. P., & Lyke, R. L. (1987) *Chem. Phys. Lett. 136*, 247–251.
Press, W. H., Flannery, B. P., Teukolsky, S. A., & Vetterling, W. T. (1986) in *Numerical Recipes*, pp 191–225, Cambridge University Press, Cambridge, U.K.
Reutimann, H., Straub, B., Luisi, P. L., & Holmgren, A. (1981) *J. Biol. Chem. 256*, 6796–6803.
Ricci, R. W. (1970) *Photochem. Photobiol. 12*, 67–75.
Rigler, R., & Ehrenberg, M. (1976) *Q. Rev. Biophys. 9*, 1–19.
Rigler, R., Claesens, F., & Lommaka, G. (1984) in *Ultrafast Phenomena IV* (Auston, D. H., & Eisenthal, K. B., Eds.) pp 472–476, Springer, Berlin.
Rigler, R., Claesens, F., & Kristensen, O. (1986) *Anal. Instrum. 14*, 525–546.
Ross, J. B. A., Laws, W. R., Buku, A., Sutherland, J. C., & Wyssbrod, H. R. (1986) *Biochemistry 25*, 607–612.
Roy, R., & Mukherjee, S. (1987) *Chem. Phys. Lett. 140*, 210–214.
Slaby, I., & Holmgren, A. (1979) *Biochemistry 18*, 5584–5591.
Smoluchowski, M. (1917) *Z. Phys. Chem. 92*, 129.
Steiner, R. F., & Kirby, E. P. (1969) *J. Phys. Chem. 73*, 4130–4135.

Stryer, L., Holmgren, A., & Reichard, P. (1967) *Biochemistry 6*, 1016-1020.
Swadesh, J. K., Mui, P. W., & Scheraga, H. A. (1987) *Biochemistry 26*, 5761-5769.
Szabo, A. (1984) *J. Chem. Phys. 81*, 150-167.
Szabo, A. G., & Rayner, D. M. (1980) *J. Am. Chem. Soc. 102*, 554-563.
Valeur, B., & Weber, G. (1977) *Photochem. Photobiol. 25*, 441-444.
Vincent, M., Brochon, J. C., Mêrola, F., Jordi, W., & Gallay, J. (1988) *Biochemistry 27*, 8752-8761.
Wahl, P. (1979) *Biophys. Chem. 10*, 91-104.
Wahl, P. (1980) in *Time resolved spectroscopy in biochemistry and biology* (Cundall, R. B., & Dale, R. E., Eds.) pp 497-521, Plenum Press, New York.
Weber, G., & Shinitzki, M. (1970) *Proc. Natl. Acad. Sci. U.S.A. 65*, 823-830.
Weinryb, I., & Steiner, R. F. (1968) *Biochemistry 7*, 2488-2495.
Werner, T. C., & Forster, L. S. (1979) *Photochem. Photobiol. 29*, 905-914.
Wiget, P., & Luisi, P. L. (1978) *Biopolymers 17*, 167-180.

Interaction of the Local Anesthetics Dibucaine and Tetracaine with Sarcoplasmic Reticulum Membranes. Differential Scanning Calorimetry and Fluorescence Studies†

C. Gutiérrez-Merino,*,‡ A. Molina,§ B. Escudero,‡ A. Diez,‡ and J. Laynez§

Departamento de Bioquímica y Biologia Molecular y Genética, Laboratorio de Bioquímica, Facultad de Ciencias, Universidad de Extremadura, 06080-Badajoz, Spain, and Instituto de Química-Física "Rocasolano", CSIC Serrano, 119, 28006-Madrid, Spain

Received April 22, 1988; Revised Manuscript Received December 2, 1988

ABSTRACT: The local anesthetics dibucaine and tetracaine inhibit the (Ca^{2+} + Mg^{2+})-ATPase from skeletal muscle sarcoplasmic reticulum [DeBoland, A. R., Jilka, R. L., & Martonosi, A. N. (1975) *J. Biol. Chem. 250*, 7501-7510; Suko, J., Winkler, F., Scharinger, B., & Hellmann, G. (1976) *Biochim. Biophys. Acta 443*, 571-586]. We have carried out differential scanning calorimetry and fluorescence measurements to study the interaction of these drugs with sarcoplasmic reticulum membranes and with purified (Ca^{2+} + Mg^{2+})-ATPase. The temperature range of denaturation of the (Ca^{2+} + Mg^{2+})-ATPase in the sarcoplasmic reticulum membrane, determined from our scanning calorimetry experiments, is ca. 45-55 °C and for the purified enzyme ca. 40-50 °C. Millimolar concentrations of dibucaine and tetracaine, and ethanol at concentrations higher than 1% v/v, lower a few degrees (°C) the denaturation temperature of the (Ca^{2+} + Mg^{2+})-ATPase. Other local anesthetics reported to have no effect on the ATPase activity, such as lidocaine and procaine, did not significantly alter the differential scanning calorimetry pattern of these membranes up to a concentration of 10 mM. The order parameter of the sarcoplasmic reticulum membranes, calculated from measurements of the polarization of the fluorescence of diphenylhexatriene, is not significantly altered at the local anesthetic concentrations that shift the denaturation temperature of the (Ca^{2+} + Mg^{2+})-ATPase. It has been found, however, that the intrinsic fluorescence of these membranes is largely quenched by these local anesthetic concentrations and that this quenching of the intrinsic fluorescence can be adequately fitted to the theoretical energy-transfer prediction using the membrane/water partition coefficients determined in this study. It is suggested that the shift of the denaturation temperature of the (Ca^{2+} + Mg^{2+})-ATPase by these anesthetics, and likely the inhibition of this activity, is related to the progressive disruption of the lipid annulus by these drugs.

A basic question underlying the studies focused on the molecular mechanism of anesthesia is the chemical nature of the anesthetic binding centers. From this perspective, it is to be recalled that previous attempts directed to support the hypothesis that perturbation of the lipid bilayer structure can account for the functional alterations linked to anesthesia have failed so far in providing major structural changes at physiologically relevant concentrations of anesthetics (Franks & Lieb, 1982; Dodson & Moss, 1984). Alternatively, it had been suggested that proteins can provide the binding sites for anesthetics with sufficient specificity and affinity (Franks & Lieb, 1982, 1986; Dodson & Moss, 1984). Because of the relatively high hydrophobic properties of these drugs, these binding sites must be hydrophobic. This and the well-known strong correlation between anesthetic potency and solubility of anesthetics in lipid bilayers suggest the possibility that the interaction of these drugs with hydrophobic binding sites in membrane proteins could be involved in the perturbations of cellular excitability produced at their pharmacological doses. In this regard, it is to be noted that several recent studies have shown

† This work has been supported by Grant 2813/13 from the Spanish CAICYT and by a grant from the Fondo de Investigaciones Sanitarias de la Seguridad Social. A preliminary account of this work was presented at the 9th International Biophysics Congress, Jerusalem, Israel, Aug 1987.

* To whom correspondence should be addressed.
‡ Universidad de Extremadura.
§ Instituto de Química-Física.

0006-2960/89/0428-3398$01.50/0